2021

The Formation of Prenucleation Clusters for Calcium Fluoride

Taylor M. Muterspaw
Wright State University

THE FORMATION OF PRENUCLEATION CLUSTERS FOR CALCIUM FLUORIDE

A Thesis submitted in partial fulfillment of the
requirements for the degree of
Master of Science

by

TAYLOR M. MUTERSPAW

B.S., Wright State University, 2019

2021

Wright State University

WRIGHT STATE UNIVERSITY

GRADUATE SCHOOL

July 29, 2021

I HEREBY RECOMMEND THAT THE THESIS PREPARED UNDER MY SUPERVISION BY Taylor M. Muterspaw ENTITLED The Formation of Prenucleation Clusters for Calcium Fluoride BE ACCEPTED IN PARTIAL FULFILLMENT OF THE REQUIREMENTS FOR THE DEGREE OF Master of Science.

_____

Steven Higgins, Ph.D.
Department of Chemistry
College of Science and Mathematics

_____

Audrey McGowin, Ph.D., Chair
Department of Chemistry
College of Science and Mathematics

Committee on Final Examination:

_____

Steven Higgins, Ph.D.

_____

Ioana Pavel, Ph.D.

_____

David Dolson, Ph.D.

_____

Barry Milligan, Ph.D.
Vice Provost for Academic Affairs
Dean of the Graduate School

ABSTRACT

Muterspaw, Taylor M. M.S., Department of Chemistry, Wright State University, 2021. The Formation of Prenucleation Clusters for Calcium Fluoride.

There have been limited studies on the analysis of the nucleation and precipitation behind calcium fluoride. Earlier studies support a nucleation mechanism in agreement to classical nucleation theory (CNT) in which a surface nucleation mechanism is required for calcium fluoride. This experiment devised using the ISE method to calcium fluoride to find evidence of a nucleation mechanism like that of calcium carbonate (prenucleation cluster pathway). The potential and pH were recorded versus time and the potential data was converted to n_{Ca}^{2+} data of free calcium ions. It was determined that there was evidence of a similar nucleation mechanism for calcium fluoride due to a similar n_{Ca}^{2+} curve being produced. It was also proven that ion pairing of the reaction cell was not a major factor to our experiments by calculations and analysis. The formation constants, K_{ip}, for CaF^{+} were found to be 3800% higher than the literature value. This experiment indicates that a similar mechanism can occur for calcium fluoride, but further analysis is needed to confirm this.

TABLE OF CONTENTS

LIST OF FIGURES

LIST OF TABLES

I. INTRODUCTION

Crystallization is one of the least understood yet vital processes of the natural world.[1] What has been of most interest in recent years is elucidating the mechanisms behind the crystallization process. Scientists for years have been trying to understand these mechanisms of crystallization. One of the most important steps behind crystallization is nucleation.[1] Nucleation is defined as the formation of the first embryo in a supersaturated system (leading to the formation of a crystalline system).[1] In the real world, there are many applications involving nucleation, such as the crystallization of proteins, purification of pharmaceutical drugs, the manufacturing of food additives, scale deposits in oil production, and the skeletal growth of corals in the ocean (biomineralization). The nucleation of minerals has been of interest in the scientific community: mainly to discover the pathway(s) that the mineral system takes towards nucleation. As of now, there is no defined answer on the specific pathway to nucleation mainly due to the difficulty in studying nucleation of these crystalline systems at the nanoscale.

The first dominant nucleation theory proposed was Classical Nucleation Theory (CNT) derived by Becker and Doring in the 1930s that was influenced from an experiment by Volmer and Weber involving water droplets formed from water vapor at critical sizes.[2-4] CNT was originally based upon the ideas of the thermodynamics behind nucleation of heterogeneous mixtures by J. W. Gibbs.[5-6]

CNT assumes that the bulk energy of a premature nucleus is the driving force towards nucleation.[2] The bulk energy balances out energy costs due to the formation of a phase interface. This phase interface consists of a critical nucleus with the same macroscopic properties.[2,7] The critical nucleus must have a radius that exceeds the critical radius to further growth.[2] After that, the attachment of atoms/molecules/nuclei to that first cluster will result in the start of the formation of a lattice. Nuclei that exceed the critical radius will grow larger in solution and not dissolve.[2] Figure 1 shows the free energy versus radius of nuclei according to CNT.

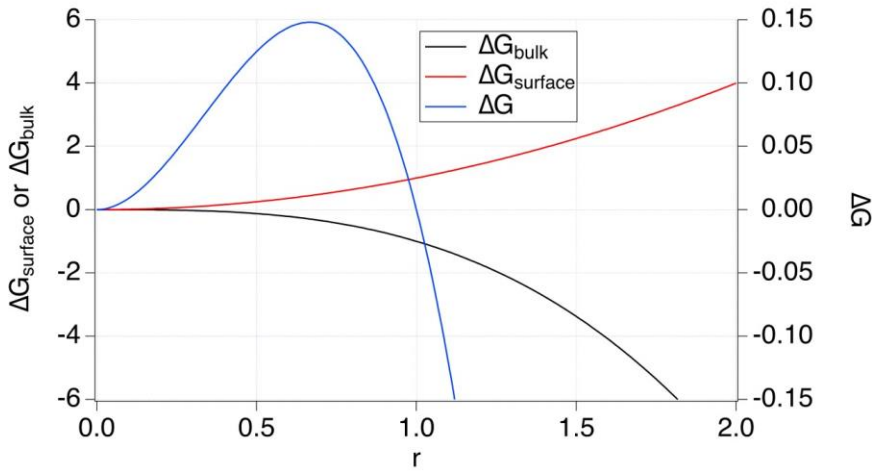

Figure 1 shows the free energy versus radius of nuclei from CNT. The surface energy (red) and the bulk energy (green) result in the surface generation (blue trace) that is balanced by the bulk energy at the critical radius.

The critical nucleus, resulted from the energy costs between the bulk energy and surface energy in Figure 1, can thermodynamically only occur in stochastic fluctuations at the microscopic level.[2] The drop in the Gibbs energy due to growing the nucleus will result in additional atoms/molecules being added spontaneously to the lattice.[7] The difference between the bulk energy and the surface energy will result in the nuclei being

stable on unstable depending on the size.[7] Nuclei that are smaller than the critical radius are thermodynamically unstable and dissolve in solution.[2] The critical size can also affect the probability of nucleation, in which a smaller critical size will result in an increased likeliness of nucleation.[7] After the formation of some critical nuclei, growth of the nuclei would proceed, eventually forming a crystalline solid. This process can occur for either homogenous nucleation or heterogenous nucleation (nucleation on a foreign surface). The free energy of the homogenous nucleation can be expressed by Equation 1 below:[8]

$$\Delta G = \frac{-4\pi r^3}{3v} KTln(S) + 4\pi r^2\sigma \qquad (1)$$

Where ΔG is the Gibbs energy given by the bulk energy, r is the radius of a nucleus, v is the volume of a single molecule, k is the Boltzmann constant, T is the absolute temperature, S is the vapor supersaturation ratio ($S = P/P^*$), and σ is the surface energy of the established phase interface.[8] Equation 1 is also relevant to crystallization of ionic solids where $S = Q/K_{sp}$. It is important to note that equation (1) pertains to a spherical nucleus.[8] The Gibbs energy of a nucleus is dependent on the size of the nucleus.[8]

A critical nucleus needs a radius at the critical size to exceed the nucleation energy barrier, which is shown by equation (2):[8]

$$\Delta G^* = \frac{16\pi\sigma^3 v^2}{3K^2T^2\ln(S)^2} \qquad (2)$$

The nucleation barrier can be substituted into a form of the Arrhenius equation to calculate the nucleation rate shown in equation (3):[8]

$$J = Ae^{\left(-\frac{\Delta G^*}{KT}\right)} \quad (3)$$

Where *A* is the prefactor (determined from kinetics) and *J* is the nucleation rate.[8] The key factors of interest to the nucleation research is the Gibbs energy of formation of the cluster, the cluster size, and the nucleation rate.[8]

Over the past few decades, CNT has been considered as being a flawed theory due to recent studies. These studies have brought the consideration of non-classical nucleation pathways in contrast to CNT. Some examples of non-classical nucleation pathways include liquid-liquid phase separation, two-step nucleation, and prenucleation clusters (PNC) for different mineral systems. Faatz et al.[9] proposed that a liquid-to-liquid phase forms for the calcium carbonate system in which two layers are formed during nucleation, one of low concentration and one of high concentration. Frenkel[10] proposed a two-step nucleation pathway for the crystallization of proteins. Gebauer et al.[11] proposed the prenucleation cluster pathway for calcium carbonate in undersaturated and supersaturated systems.

The experiment of Gebauer et al.[11] on calcium carbonate was a crucial step towards understanding the mechanism(s) behind nucleation for a mineral system. Figure 2 shows the data for the experiment plotted as n_{Ca}^{2+} (μmol) versus time (s) at pH = 9.25 (calcium carbonate nucleation is more favored at alkaline pH levels).[11]

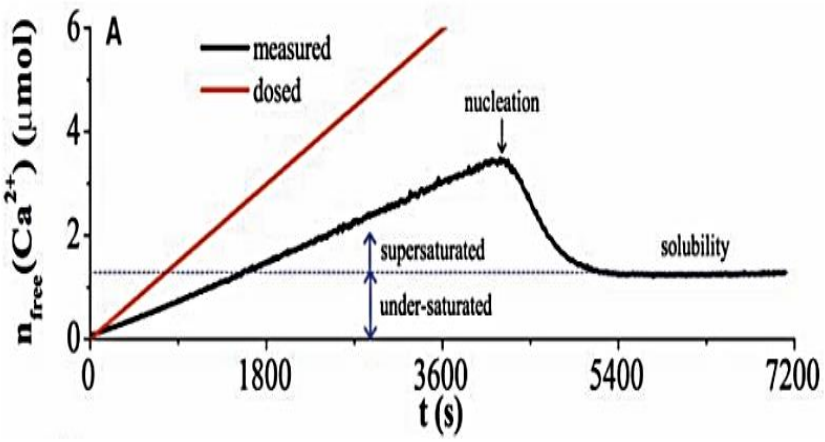

Figure 2 shows the $n_{Ca^{2+}}$ of free calcium ions (µmol) versus time (s) for Gebauer et al's experiment at pH = 9.25 (black line).[11] The dosage line (red line) represents the $n_{Ca^{2+}}$ of free calcium ions based on calculations.[11] Reprint granted permission from The American Association for the Advancement of Science.

What Gebauer et al.[11] observed from Figure 2 is that the n_{Ca}^{2+} measured was less compared to the actual dosage line for Ca^{2+}, implying that the calcium ions are binding to the carbonate ions in solution. The steady increase of the measured n_{Ca}^{2+} in the prenucleation stage was due to the added calcium titrant.[11] It was also discovered that these clusters formed two amorphous calcium carbonate (ACC) phases dependent on the pH.[11] This was further proven by Gebauer et al.[11] using analytical ultracentrifugation (AUC) where large clusters were discovered in the late prenucleation stage and early post-nucleation stage.

It was concluded that prenucleation clusters do exist for calcium carbonate and it was suggested that the nucleation process for these stable clusters was established via aggregation in contrast to CNT. In CNT, these clusters will continue to grow after

exceeding the critical cluster size and form metastable clusters after exceeding the change in Gibbs energy.[11] Figure 3 shows Gibbs energy versus the reaction coordinate.[11]

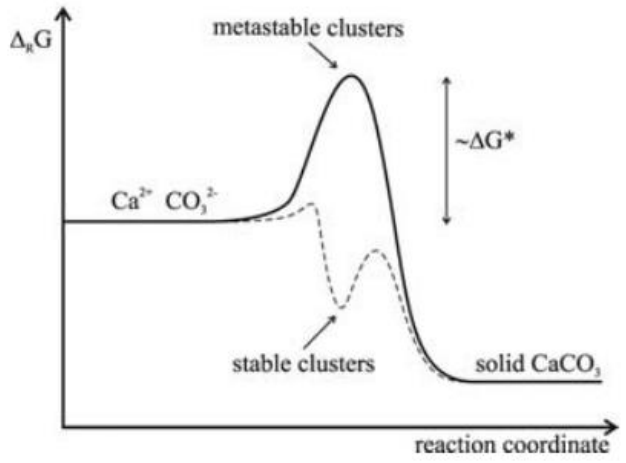

Figure 3 shows the Gibbs free energy versus the reaction coordinate for calcium carbonate according to CNT (solid line) versus the PNC pathway (dashed line).[11] Reprint granted permission from The American Association for the Advancement of Science.

For in the non-classical view in Figure 3, these stable clusters form with a minimum in the Gibbs energy due to the existence of a stable equilibrium cluster.[11] This also contrasts to CNT to the fact that metastable clusters in the prenucleation stage are a rare species.[2,11] For the PNC pathway, these clusters are stable and can exist in an undersaturated system. The PNC pathway can be seen by Figure 4 below.

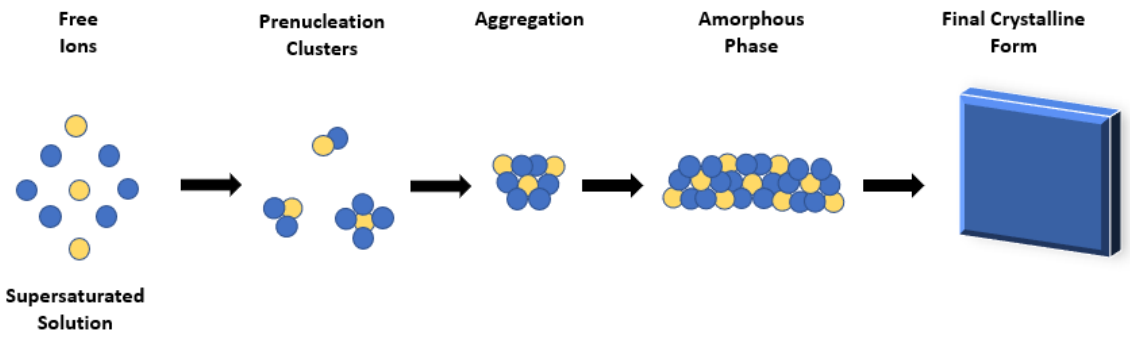

Figure 4 shows the PNC pathway as proposed by Gebauer et al[11] where these stable clusters were formed via aggregation.

After these prenucleation clusters form, aggregates occur which then construct an amorphous phase in supersaturation of the system and then a final crystalline form is established. The experiment of Gebauer et al.[11] was a pivotal step towards providing the evidence of PNCs as well as a direction towards a non-classical description of nucleation such as Figure 4.

There have also been investigations of nucleation for other mineral systems (such as calcium phosphate and hematite) and proteins.[10,12-13] Understanding the nucleation of various mineral systems can help scientists further understand the chemistry of this process. This paper specifically involves testing for evidence of PNCs for calcium fluoride (CaF_2).

Calcium fluoride (CaF_2), or also known as the mineral fluorite, has been used in optical devices and can also occur as an intermediate phase in the use of toothpaste for oral hygiene.[14] There have been limited studies on the nucleation and precipitation of

calcium fluoride in the past decades. Early studies pertained to understanding the kinetics of crystallization for calcium fluoride but do not test CNT specifically.[14-16]

Beckerbt et al[17] investigated the formation of different calcium fluoride cluster ions using spark source mass spectrometry and laser ablation ICP-MS using a solid crystalline sample. The calcium fluoride cluster abundance distributions agreed well for both methods.[17] Madsen[18] carried out a turbidimetric experiment with calcium fluoride in which concluded that the nucleation rate versus supersaturation for calcium fluoride supported CNT at first, but one discrepancy was found in which the absolute rate of nucleation was lower than the predicted amount by CNT by many orders of magnitude. This was due to an overestimation of the rate of growth in the postcritical nuclei, indicating future experimentation being needed for calcium fluoride.[18]

Kügler and Kind[19] analyzed the precipitation of calcium fluoride (and strontium fluoride) by using a dynamic light scattering method to measure particle size distributions experimentally and on calculations by theory; it was observed that the results were concurrent with CNT in those the experimental and theoretical results agreed well with each other and that interfacial energy was the only fitting parameter. Previous research in testing the validity of CNT or a non-classical mechanism seem to be sparse for calcium fluoride. Previous studies mentioned have treated nucleation of fluorite using the classical theory in contrast to a non-classical theory like that used to describe calcium carbonate formation.

The purpose of this experiment was to see if calcium fluoride had a similar nucleation mechanism to that of calcium carbonate. Evidence of this possible mechanism and varying the [F^-] was tested by using the ISE method through the titration of fluoride solutions with calcium titrant throughout the formation of calcium fluoride.

II. MATERIALS AND METHODS

1. *Materials and Solution Preparation –*

Solutions of calcium (Fisher Scientific) were prepared from a calcium chloride dihydride stock (Fisher Scientific). The carbonate and bicarbonate solutions (reproducing Gebauer's experiment) were prepared from sodium carbonate and sodium bicarbonate stocks (Fischer Scientific, ACS certified) and the sodium hydroxide solution was also prepared from a sodium hydroxide stock (Fischer Scientific, ACS certified). Fluoride solutions were made from a sodium fluoride stock (Sigma Aldrich, ≥99% certified). The sodium hydroxide solution was also prepared from a sodium hydroxide stock (Fischer Scientific, ACS certified). All solutions were prepared with high quality water (HQ) (Millipore). Each calcium standard and fluoride solution had 1.00 mL of the ionic strength adjuster (ISA, 4 M KCl) added to increase the ionic strength for better potential readings. The pH buffers used to calibrate the pH electrode were pH = 7.00 (Fischer Scientific, certified pH = 6.99-7.01 at 25 ºC, color coded yellow) and pH = 10.00 (Fisher Scientific, certified pH = 9.98-10.02 at 25 ºC, color coded blue).

2. *Reproducing Gebauer's Experiment –*

It was crucial to make sure that Gebauer's experiment could be reproduced before doing an experiment with calcium fluoride, so that it could be confirmed that Gebauer's experiment was possible in producing prenucleation clusters for calcium carbonate. The potential was recorded with an Oakton by Cole-Parmer calcium combination ion selective electrode (ISE) and the pH was recorded by a Vernier pH electrode. First, the

ISE had to be calibrated by recording the potential values of the following calcium standards (standards were stirred with a stir bar on a stir plate): 1 ppm, 10 ppm, 100 ppm, and 1000 ppm. The ISE had to be soaked in HQ water for about 30 minutes before the calibration process. The potential was recorded by a Thermo Scientific Orion Star A211 pH meter. After recording the potential values versus the log concentration of each calcium standard in Microsoft Excel (and plotted), a trendline was imposed on the data; an equation of the trendline and the R^2 value of the data was also determined. The calibration would be determined successful if the R^2 value was 0.99 or higher.

The next step was to calibrate the pH electrode by immersing the pH electrode in pH buffers of 7 (yellow) and 10 (blue) for about a minute each separately (buffers stirred with stir bar on a stir plate). After 1 minute in the buffer, the literature pH value was logged into the LoggerLite software (version 1.9.3). The data collection setup for the pH electrode was set to record the pH every 5 seconds.

After calibrating both electrodes, the reaction cell was setup, and the experiment was performed (see *Appendix A – Calcium Carbonate Experiment* for results). The 10 mM carbonate/bicarbonate buffer in the beaker was titrated with 2.6 mL of 10 mM calcium (NaOH was also slowly titrated into the buffer to keep the pH at 9.5 since nucleation occurs at more alkaline pH values) while stirred. The flow rate for the titrant was set to 0.020 mL/min on the systematic pump (flow rate is more accurate to 0.0195±0.0005 mL/min) and helium was bubbled into the buffer to keep any extra carbon

out of the system. It is important to note that a gas washing bottle was used to saturate the helium with water vapor first before the experiment. During the experiment, the potential (Orion Star Com) and pH were recorded versus time as the titrant was added to the buffer solution by a 3 mL plastic syringe with tubing. The experiment was conducted at room temperature (23±1 ºC).

a. Sample Preparation –

   i. Calcium Standards – The calcium standards for calibration were the following concentrations: 1 ppm, 10 ppm, 100 ppm, and 1000 ppm. Standards were prepared pipetting a certain amount of the 1000 ppm calcium stock solution and diluted in 100 mL volumetric flasks with high quality (HQ) water. Exactly 50.00 mL of each standard was pipetted into a 100 mL beaker and 1.00 mL of ISA (4 M KCl) was added to adjust the ionic strength of the standards.

   ii. 10 mM carbonate/bicarbonate buffer – Bicarbonate and carbonate solutions were prepared separately in 100 mL volumetric flasks (both 10 mM). Buffer was prepared by pipetting 40.00 mL of bicarbonate and 5.92 mL of carbonate (in order for pH = 9.5) into a beaker. Exactly 1.00 mL of ISA (4 M KCl) was added to the buffer with a displacement pipet. A stir bar was also added. The buffer was then sealed with parafilm first to prevent reaction with CO_2.

iii. 10 mM calcium titrant – The titrant solution was first prepared in a 10 mL volumetric flask. Next, a 3 mL plastic syringe was rinsed twice with HQ water and then rinsed with the titrant. About 2.6 mL of the titrant was pipetted into the syringe as well as 1.00 mL of 0.01 M NaOH. The syringe was connected to a luer fitting that was connected to the tubing.

3. Experiment for Calcium Fluoride –

Experiments were conducted to determine if there were evidence of prenucleation clusters for calcium fluoride. In this experiment, 2 mL of 8 mM calcium was titrated into 50 mL of a fluoride solution; the potential and pH were recorded versus time for the titration.

After calibrating both electrodes (same procedure as the calcium carbonate experiment), the reaction cell was setup the same but with the fluoride solution instead of the carbonate/bicarbonate buffer. The reaction cell setup can be seen by Figure 5 below.

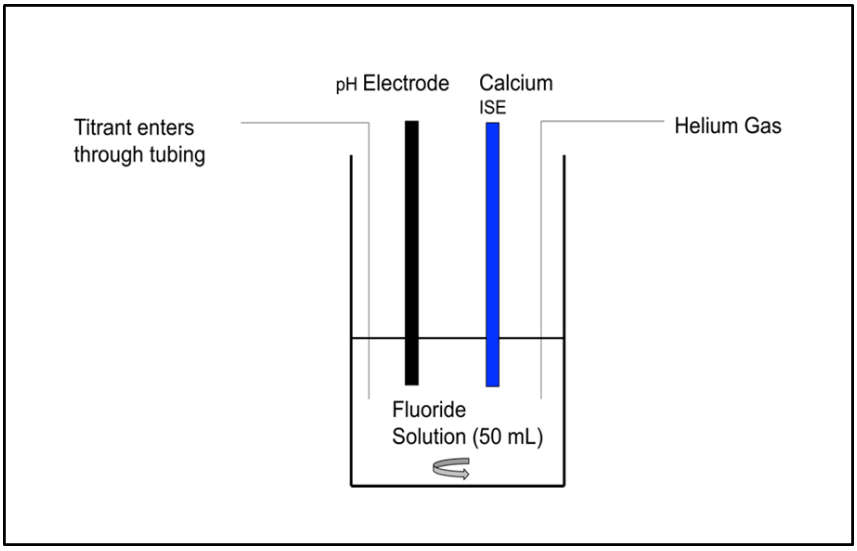

Figure 5 shows the schematic diagram for the reaction cell for the calcium fluoride experiment.

Both the calcium ISE and the pH electrode (in the reaction cell from Figure 5) were immersed in the fluoride solution first. Next, tubing was immersed into the fluoride solution as well to bubble helium gas into the fluoride solution. The helium gas needed to be bubbled into the fluoride solution also to keep extra carbon out of the reaction cell. Another length of tubing was inserted into the fluoride solution to titrate the 8 mM calcium solution. The titrant was introduced by a 3 mL syringe that was placed on a systematic pump to titrate into the solution over a long period of time. The flow rate for the titrant was set on the systematic pump as 0.025 mL/min, although through measurements, it was determined that the actual flow rate was approximately 0.0200±0.0005 mL/min. After setting up the reaction cell, the Orion Star Com and LoggerLite software was setup to record the potential (mV) and pH versus time (connected to the pH Meter) for every 5 seconds. The data collection process was

initiated without the titrant being pumped into the solution (to make sure there is no interference in the data collecting). After about 5-6 minutes, the systematic pump was then started to titrate the 2 mL of 8 mM calcium into the fluoride solution.

Triplicate runs were performed for different fluoride concentrations to observe any differences in the n_{Ca}^{2+} data. Triplicate runs were performed for the following fluoride concentrations: 12.8 mM, 19.2 mM, 25.6 mM, 38.4 mM, and 51.2 mM (Table 1). Each experiment was performed at room temperature (23 ± 1 ºC).

a. Sample Preparation –
    i. Calcium standards – The calcium standards were prepared the same as the ones in the calcium carbonate experiment.
    ii. 8 mM calcium titrant – Titrant solution was prepared the same except with a different calcium concentration.
    iii. Fluoride solution – The fluoride solution was prepared in a 100 mL volumetric flask and 50.00 mL was pipetted into a 100 mL beaker. Exactly 1.00 mL of ISA (4 M KCl) was added to the solution by a displacement pipet as well as a stir bar. The solution was then sealed with parafilm.

Table 2 shows the list of the fluoride concentrations used for each triplicate run performed for calcium fluoride.

Experiment Triplicate Run	Fluoride Concentration (mM)
1	12.80±0.03
2	19.20±0.05
3	25.60±0.06
4	38.40±0.10
5	52.60±0.13

III. RESULTS

For calcium fluoride, a series of 6 triplicate experiments were performed in which the fluoride concentration was varied for each triplicate run (the calcium titrant concentration was fixed at 8.0 M). Figure 6 shows a typical titration curve of showing ISE potential (mV) versus time.

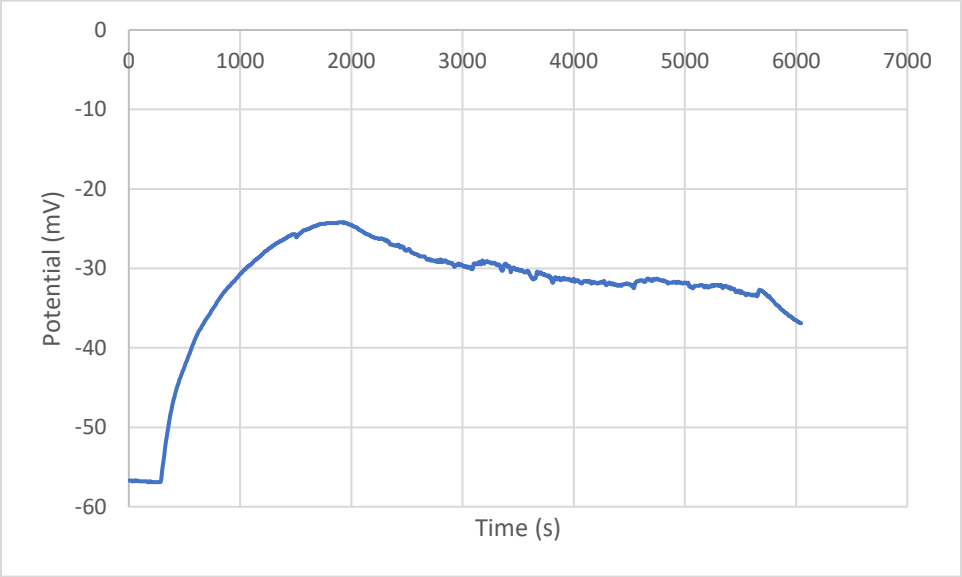

Figure 6 shows the potential (mV) versus time (s) data for the titration recorded by the calcium ISE (10-6) for [F^-] = 25.6 mM

From Figure 6, the data indicates a steady increase in the potential until reaching a peak where nucleation occurs, then a slight decline of the potential value follows, indicating that a reaction is taking place in the solution.

The titration data was converted to n_{Ca}^{2+} through the same calculations as the calcium carbonate experiment (see *Appendix A – Calcium Carbonate Experiment* and

Appendix C – Other Data Plots for Calcium Fluoride Experiment for other data plots).

Figure 7 shows a plot of the amount of free calcium ions, n_{Ca}^{2+}, versus n_{Dosed}.

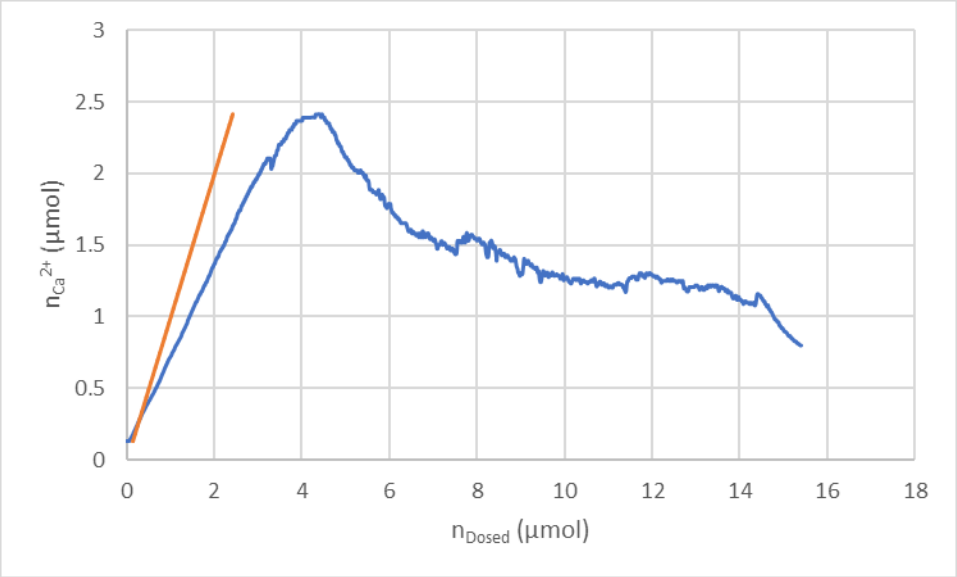

Figure 7 shows the n_{Ca}^{2+} of free calcium ions (µmol) versus n_{Dosed} (µmol) for the titration (blue line). The total dosage of calcium based on the flow rate is also shown (orange line). The was done at [F^-] = 25.6 mM.

Figure 7 indicates that the calcium ions are binding to the fluoride ions in solution, which would result in a decrease in the detection of free calcium ions; therefore, the n_{Ca}^{2+} data supports the hypothesis for the existence of prenucleation clusters of calcium fluoride. The data in Figure 6 shown is similar when compared to the titration La Mer[20] curves in Gebauer et al's[11] calcium carbonate experiment where once the n_{Ca}^{2+} curve reaches a peak, that is where nucleation occurs where the precipitation phase begins (crystal formation). Another observation was that the free Ca^{2+} was larger than the calculated equilibrium n_{Ca}^{2+}, 0.0134 µmol. The calculated equilibrium n_{Ca}^{2+} would nearly coincide with the horizontal axis and is thus not shown in Figure 6. This also considers

growth kinetics (mainly after the nucleation peak) in which the growth rate of the crystals is balanced with the rate of the pump (highly supersaturated).

The calcium fluoride experiment was performed at various fluoride concentrations to compare the n_{Ca}^{2+} curves from each concentration. A triplicate titration run was performed for each fluoride concentration. Figure 8 shows a n_{Ca}^{2+} plot with all three titration runs for $[F^-]$ = 25.6 mM.

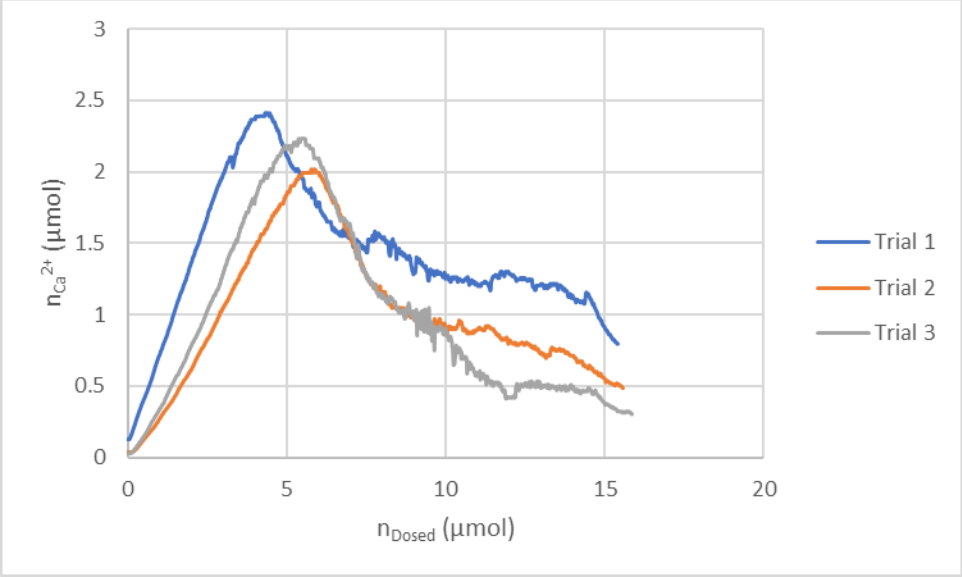

Figure 8 shows the n_{Ca}^{2+} (µmol) vs. n_{Dosed} (µmol) for a triplicate run for $[F^-]$ = 25.6 mM.

The n_{Ca}^{2+} curves in Figure 8 appear to have variation in the slopes (before peak) and peak heights (not very agreeable). One possible explanation for this could be the effect of electrode drift from the ISE. Temperature differences may have played a role as well in the variations. A series of triplicate runs were completed for the other fluoride concentrations (see *Appendix C – Other Data Plots for Calcium Fluoride Experiment*).

One observation that was made for the triplicate experiments was that as the [F^-] increased, the time for the solution to reach the critical point (nucleation stage) decreased. Another observation is that the slopes and peak heights vary with different [F^-]. From this observation, the slopes and peak heights at different fluoride concentrations (triplicate run for each [F^-]) were recorded.

One consideration for this experiment was that of CaF^+ ion pair formation. Ion pairing is defined as the partial association of opposite charged ions in a solution instead of forming the desired compound (mainly due the electrostatic attractions in solution).[21] The formation of ion pairs would result in an ISE-detected amount of Ca^{2+} that was less than the dosage of Ca^{2+}. A series of calculations were made and compared to the dosage line where concentrations of Ca^{2+}, F^-, and CaF^+ using the ISE data and the reported equilibrium constant value for CaF^+ formation (see *Appendix B – Sample Calculations*). From there, the calculated CaF^+ amount was subtracted from the total Ca^{2+} dosage line and plotted along with the dosage line and ISE data, which is shown by Figure 9 below.

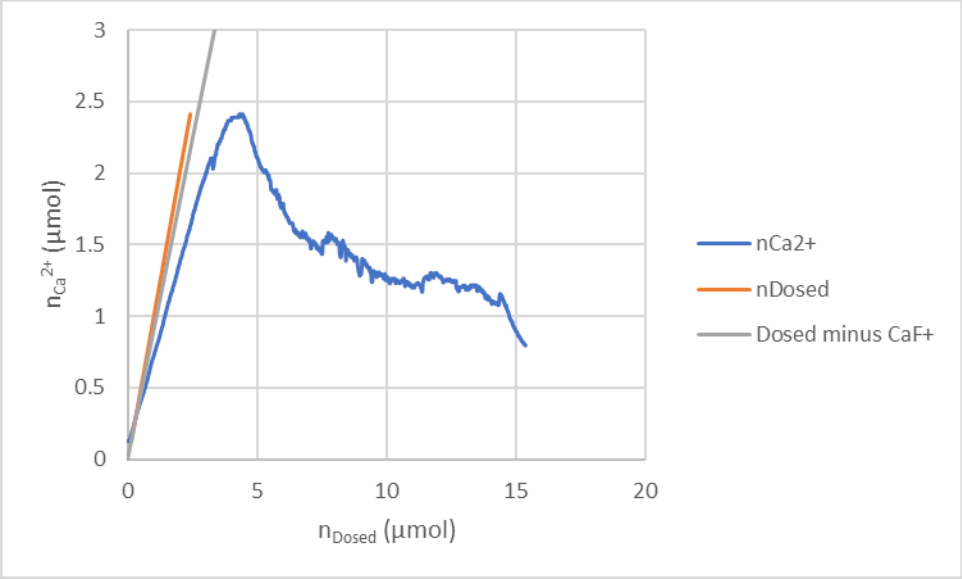

Figure 9 shows the $n_{Ca^{2+}}$ (µmol) versus n_{Dosed} for the titration run (blue line). The total dosage of calcium based on the flow rate is also shown (orange line) as well as the total Ca^{2+} dosage line after subtracting the amount of CaF^{+} (gray line).

Figure 9 shows the effect of ion pairing on the free Ca^{2+} (gray line) by subtracting the calculated amount of CaF^{+} from the total Ca^{2+} dosage data (orange line). There is a slight difference between the two lines that can be seen. The ion pairing $CaCl^{+}$ was considered as well and similar calculations were performed (see *Appendix B – Sample Calculations*). Figure 10 shows the effect of the $CaCl^{+}$ ion pairing on the dosed calcium line for the n_{Ca}^{2+} plot.

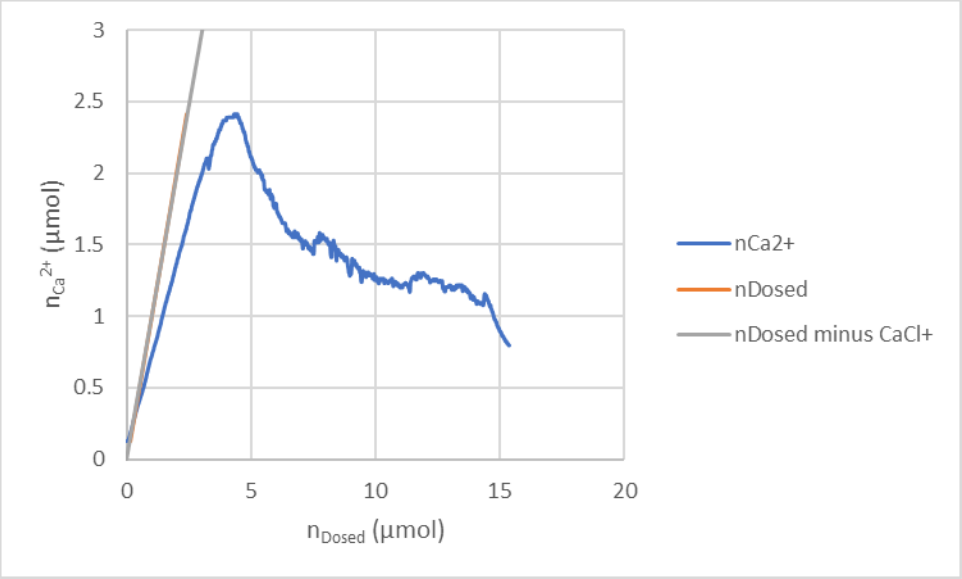

Figure 10 shows the n_{Ca}^{2+} (µmol) versus n_{Dosed} for the titration run (blue line). The total dosage of calcium based on the flow rate is also shown (orange line) as well as the total Ca^{2+} dosage line after subtracting the amount of $CaCl^{+}$ (gray line).

It can be seen from Figure 10 that the ion pairing results are similar as to CaF^{+}, where there is little variation between the dosage line (orange) and the ion pairing effect line (grey).

As an alternative method of analysis of the titration data, the equilibrium constant, K_{ip}, for CaF^{+} formation was estimated by assuming that prenucleation cluster formation does not occur. Figure 11 shows a major increase in the slope approximately around 1480 s. This correlates to the n_{Ca}^{2+} plot (Figure 7) in which the peak occurs around the same time frame.

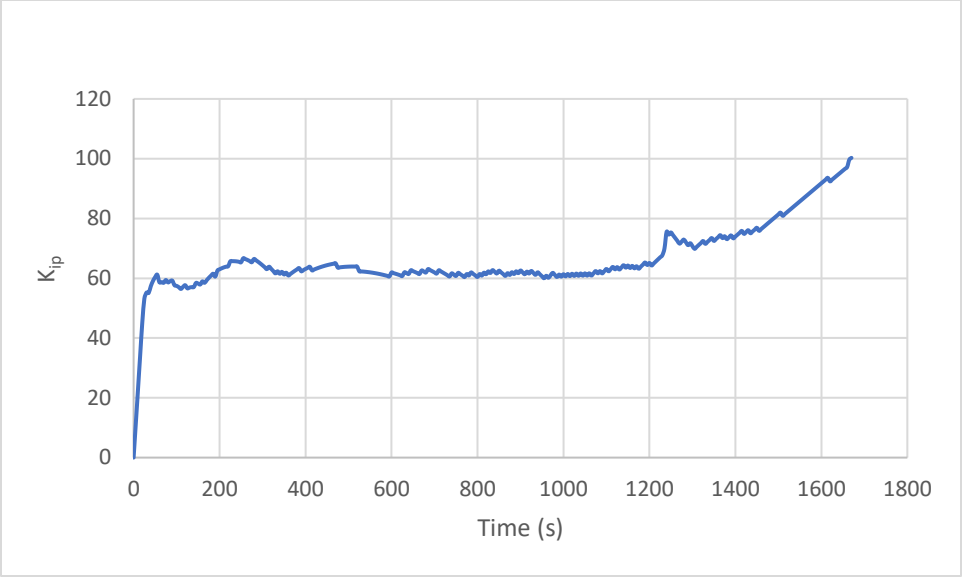

Figure 11 shows the K_{ip} for CaF^+ versus time (s) for the calcium fluoride titration for $[F^-]_{initial}$ = 25.6 mM.

The averages for the rising slopes and peak heights for each of the titrations at different fluoride concentrations were recorded for further analysis. The average equilibrium constant, K_{ip} for CaF^+ was calculated as well, assuming the only mode of Ca^{2+} consumption prior to nucleation was from ion pair formation (Figure 11). Figure 12 shows the slope versus the $[F^-]$

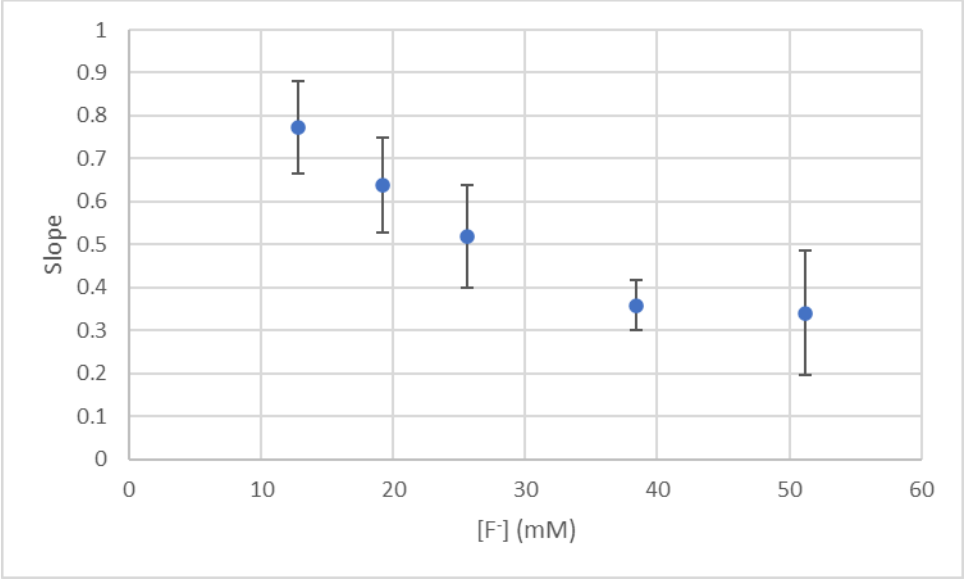

Figure 15 shows the average slope versus the [F-] for the calcium fluoride experiment.

A downward trend can be seen from Figure 12. The slope decreases as the [F-] increases. Figure 13 shows the peak height (µmol) versus [F-].

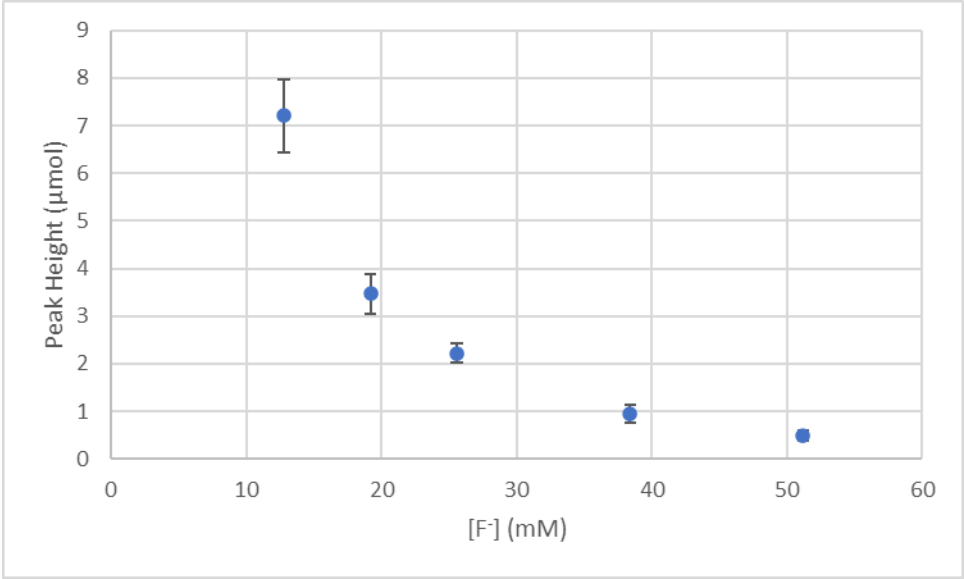

Figure 16 shows the average peak height (µmol) versus the [F-] for the calcium fluoride experiment.

A downward trend can also be seen with Figure 13 in which the peak height decreases as the [F^-] increases. Figure 14 shows the calculated average K_{ip} value versus [F^-].

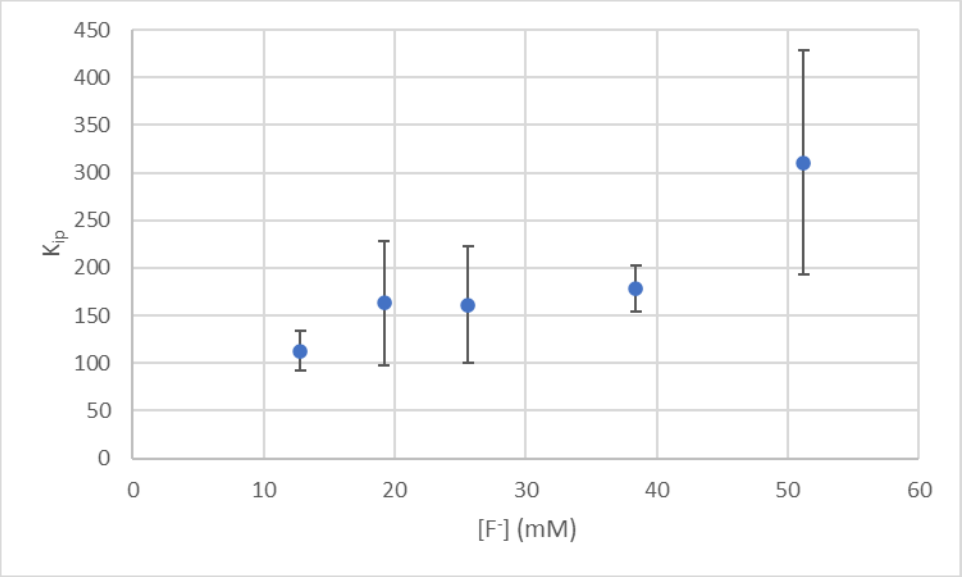

Figure 17 shows the calculated average Kip versus the [F-] for the calcium fluoride experiment.

It can be seen from Figure 14 that the K_{ip} remains mostly constant as the [F^-] increases.

At [F^-] = 12.8 mM for Figure 13 a peak was not observed for the n_{Ca}^{2+} data using the typical titrant volume; therefore, more titrant was used for this fluoride concentration (3.00 mL).

IV. DISCUSSION

The collection of evidence of PNC formation as well as the effects of key factors that control cluster formation (e.g., cluster size, temperature, concentration ratio, etc.) is crucial to the understanding of their chemistry. By performing a potentiometric titration of sodium fluoride with calcium chloride, free calcium ion concentrations were monitored and the effect of varying the calcium-to-fluoride concentration ratio was investigated.

From the calcium fluoride experiments, it was confirmed that there was evidence of PNCs forming. The n_{Ca}^{2+} plot in Figure 7 for calcium fluoride showed a La Mer curve like those observed in Gebauer et al.[11] for calcium carbonate. Evidence of the calcium ions binding to the fluoride ions in solution to produce these clusters is clear in Figure 7 where the amount of free calcium ions is well below the total amount of calcium line. For the ion pairing calculations, it was determined that ion pairing did not have a dramatic effect in our experiment. The ion pairing curve in Figure 9 shows a small change in the theoretical n_{Ca}^{2+} data compared to the amount of total calcium, with the observed n_{Ca}^{2+} data markedly below the theoretical prediction.

This finding contrasts to previous studies of calcium fluoride. The findings of Madsen[18] for calcium fluoride precipitation supported classical nucleation. The nucleation frequency for calcium fluoride tend to increase as the function of supersaturation increased. There was one discrepancy in their experiment in which the

absolute value of the nucleation rate was of orders of magnitude lower than predicted by CNT.[18] This called for further investigation for calcium fluoride. Kügler and Kind[19] carried out experiments whose results also agreed more with CNT kinetics due to the evidence of primary particles forming for calcium fluoride and strontium fluoride. The mean particle size versus the initial supersaturation for calcium fluoride agreed well with calculated results by CNT (only when a diluted surfactant solution was added) by making the interfacial energy as a fitting parameter.[19]

The above studies involve using a light scattering approach in contrast to the ISE method. The ISE yields the electrode potential, and by extension, the concentration of free calcium in the prenucleation stage compared to the light scattering methods which in principle only detect particles in the post nucleation stage. A laser pointer was used for the reaction cell after the experiment and scattering was observed, indicating that there were particles in the reaction cell post nucleation (see *Appendix D – Laser Pointer Experiment for Calcium Fluoride*). The ISE method was a better approach for our experiment in determining if the nucleation pathway for calcium fluoride was similar to calcium carbonate.

Our experimental investigations revealed in Figure 6 that changing the fluoride concentration affected the n_{Ca}^{2+} curve. As the $[F^-]$ increased, the slope (Figure 12) for the prenucleation stage decreases and the height of the curve at the nucleation point decreases. These observations can be explained by considering that at higher [F-] there is

more fluoride in solution for the calcium ions to bind to (either through ion pairing or clustering) and therefore there is less free calcium to elicit a response of the ISE. This would also result in the n_{Ca}^{2+} values being lower compared to the total Ca^{2+} dosage line as more calcium ions were binding in solution. The peak height (Figure 13) also decreased as the $[F^-]$ increased, which is congruent with our findings since the nucleation peak would be reached quicker as there are more fluoride ions to bind to. These trends in the slope and the peak height further suggest evidence of supersaturation of the system.

It was determined that ion pairing did not significantly deplete the solutions of free calcium ions in our experiments according to Figure 9 and the K_{ip} values in Figure 14. There was little difference in comparing the calculated CaF^+ subtracted from total calcium dosage line to the amount of n_{Ca}^{2+}. While ion pairing does reduce the amount of free Ca^{2+}, it does not account for the ISE-detected amount of free Ca^{2+}. For $CaCl^+$, it was determined according to Figure 10 that there was little ion pairing effect for the reaction cell as well by using similar calculations (see *Appendix B – Sample Calculations).*

The K_{ip} for CaF^+ was calculated at each fluoride concentration (Figure 14). The purpose of calculating the K_{ip} was to further disprove ion pairing having a major impact in the experiment. The average K_{ip} values increased with an increase in $[F^-]$ for each experiment in the prenucleation stage. It is important to note that the K_{ip} values were calculated by taking the average of the K_{ip} data where the K_{ip} plot was roughly constant. Also, the K_{ip} values are much larger compared to the literature value for CaF^+ (e.g. K_{ip} =

161±60 for [F^-] = 25.6 mM), which is 4.27[22]. This also indicates evidence of cluster formation.

This also is more evidence that there is cluster formation in the reaction cell due to the increase of the K_{ip}. The drastic increase in the slope shortly prior to nucleation can be seen in Figure 11 (the slope of the data curve increases around approximately after 1200 s). The drastic increase in the slope indicates a dynamic change in the reaction quotient of the system; the reaction cell undergoes a different mechanism that cannot be described as a simple ion pair such as CaF^+. The post nucleation stage of the reaction undergoes a new mechanism all together, where nucleation begins after the nucleation peak is reached.

V. CONCLUSION

The purpose of this experiment was to test if the formation mechanism of calcium fluoride was like that of calcium carbonate by the means of PNC pathway. The n_{Ca}^{2+} data of the free calcium ions in solution provided evidence for the existence of a similar nucleation mechanism due to the data being less compared to the calculated total calcium line. Our analysis indicated that as the $[F^-]$ increased, the linear slope showed that there is an equilibrium dictating free calcium ions due to more fluoride ions available to bind to. This is also more evident in the K_{ip} values calculated. Ion pairing was considered to not be a major hinderance in our experiment by having little effect on the dosed calcium line n_{Ca}^{2+} data and the K_{ip} values calculated; further proving that clustering is occurring in solution. It can be suggested that the mechanism for nucleation can be the PNC pathway via aggregation like calcium carbonate, but future analysis would be needed to confirm the existence of PNCs for calcium fluoride, such as AUC or Scanning Electron Microscopy (SEM). This model system proposed in this paper can also act as a lead way for other mineral systems as well as help further understand the chemistry behind nucleation.

REFERENCES

(1) Lutsko, J. F. How Crystals Form: A Theory of Nucleation Pathways. *Sci. Adv.* **2019**, *5* (4), 1–9. https://doi.org/10.1126/sciadv.aav7399.

(2) Gebauer, D.; Cölfen, H. Prenucleation Clusters and Non-Classical Nucleation. *Nano Today*. December 2011, pp 564–584. https://doi.org/10.1016/j.nantod.2011.10.005.

(3) Becker, W., Doring, R. ~eron~ut~~s. *Natl. Advis. Comm. Aeronaut.* **1935**, *1374*, 719–752.

(4) Volmer, M.; Weber, A. Z. *Zeitschrift für Physikalische Chemie* **1926**, *119*, 277–301.

(5) Gibbs, J. W. Heidelberger Texte Zur Mathematikgeschichte. *Trans. Connect. Acad. Arts Sci.* **1903**, *3* (1874–1878), 108–248.

(6) Gibbs, J. W. Heidelberger Texte Zur Mathematikgeschichte. *Trans. Connect. Acad. Arts Sci.* **1903**, *3* (1874–1878), 343–524.

(7) De Yoreo, J. J.; Vekilov, P. G. Principles of Crystal Nucleation and Growth. *Rev. Mineral. Geochemistry* **2003**, *54* (1), 57–93. https://doi.org/10.2113/0540057.

(8) Karthika, S.; Radhakrishnan, T. K.; Kalaichelvi, P. A Review of Classical and Nonclassical Nucleation Theories. *Cryst. Growth Des.* **2016**, *16* (11), 6663–6681.

https://doi.org/10.1021/acs.cgd.6b00794.

(9) Faatz, B. M.; Gröhn, F.; Wegner, G. Amorphous Calcium Carbonate : Synthesis and Potential Intermediate in Biomineralization. *Adv. Mater.* **2004**, *16* (12), 996–1000. https://doi.org/10.1002/adma.200306565.

(10) Frenkel, D. Enhancement of Protein Crystal Nucleation by Critical Density Fluctuations. *Science (80-.).* **1997**, *277* (5334), 1975–1978. https://doi.org/10.1126/science.277.5334.1975.

(11) Gebauer, D.; Völkel, A.; Cölfen, H. Stable Prenucleation Calcium Carbonate Clusters. *Science (80-.).* **2008**, *322* (5909), 1819–1822. https://doi.org/10.1126/science.1164271.

(12) Garcia, N. A.; Malini, R. I.; Freeman, C. L.; Demichelis, R.; Raiteri, P.; Sommerdijk, N. A. J. M.; Harding, J. H.; Gale, J. D. Simulation of Calcium Phosphate Prenucleation Clusters in Aqueous Solution: Association beyond Ion Pairing. *Cryst. Growth Des.* **2019**, *19* (11), 6422–6430. https://doi.org/10.1021/acs.cgd.9b00889.

(13) Scheck, J.; Fuhrer, L. M.; Wu, B.; Drechsler, M.; Gebauer, D. Nucleation of Hematite: A Nonclassical Mechanism. *Chem. - A Eur. J.* **2019**, *25* (56), 13002–13007. https://doi.org/10.1002/chem.201902528.

(14) Shyu, L.; Nancollas, G. The Kinetics of Crystallization of Calcium Fluoride. A

New Constant Composition Method. *Croat. Chem. Acta* **1980**, *53* (2), 281–289.

(15) Møller, H.; Madsen, H. E. L. Growth Kinetics of Calcium Fluoride in Solution. *J. Cryst. Growth* **1985**, *71* (3), 673–681. https://doi.org/10.1016/0022-0248(85)90376-8.

(16) Perez, L. A., Nancollas, G. H. PII 0166-6622(91)80017-I Elsevier Enhanced Reader.Pdf. *Colloids and Surfaces* **1991**, *52*, 231–240. https://doi.org/10.1016/0166-6622(91)80017-I.

(17) Beckerbt, S.; Seifert, G.; Kaschnera, R. Theoretical and Mass Spectrometric Investigations of the Formation of Calcium Fluoride Cluster Ions. *Int. J. Mass Spectrom.* **1998**, *176* (1–2), 103–111. https://doi.org/10.1016/S1387-3806(98)14020-4.

(18) Lundager Madsen, H. E. Turbidimetric Study of Fluorite Nucleation in Solution. *J. Colloid Interface Sci.* **2007**, *307* (2), 469–476. https://doi.org/10.1016/j.jcis.2006.11.001.

(19) Kügler, R. T.; Kind, M. On Precipitation of Sparingly Soluble Fluoride Salts. *Cryst. Growth Des.* **2018**, *18* (2), 728–733. https://doi.org/10.1021/acs.cgd.7b01115.

(20) LaMer, V.; Dinegar, R. H. *J. Am. Chem. Soc.* **1950**, *72* (11), 4847–4854. https://doi.org/10.1097/00007611-192203000-00016.

(21) Marcus, Y.; Hefter, G. Ion Pairing. *Chem. Rev.* **2006**, *106* (11), 4585–4621. https://doi.org/10.1021/cr040087x.

(22) Harris, D. C. In *Quantitative Chemical Analysis*; W. H. Freeman and Company: New York, NY, **2010**, p AP31.

Appendix A

Calcium Carbonate Experiment

Before running the titration, a calibration had to be made for the calcium ISE with the calcium standards. Figure S1 shows the calibration curve of potential (mV) vs. log(concentration) (ppm) for the calibration of the ISE.

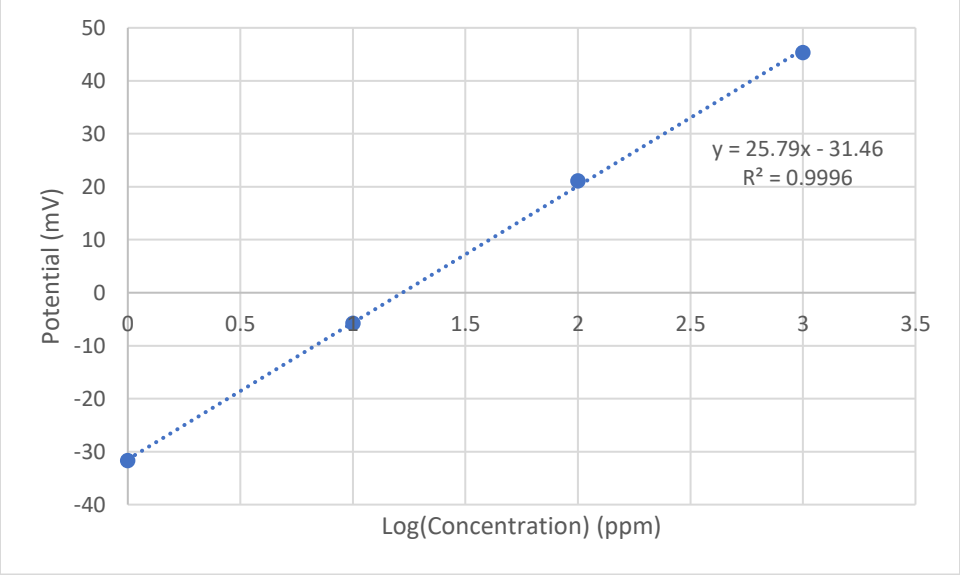

Figure S1 shows the calibration curve of potential (mV) versus log(concentration) (ppm) for the calcium ISE. The equation of the line and R^2 value are also shown.

According to Figure S1, the R^2 value was 0.9997, indicating that the calibration was successful; the equation of the line was determined to be y = 23.8x – 30.5, which would be used later to convert the titration data to n_{Ca}^{2+} (µmol).

After the experiment, the potential and pH data were saved as CSV files. Figure S2 shows the pH versus time (s) for the experiment.

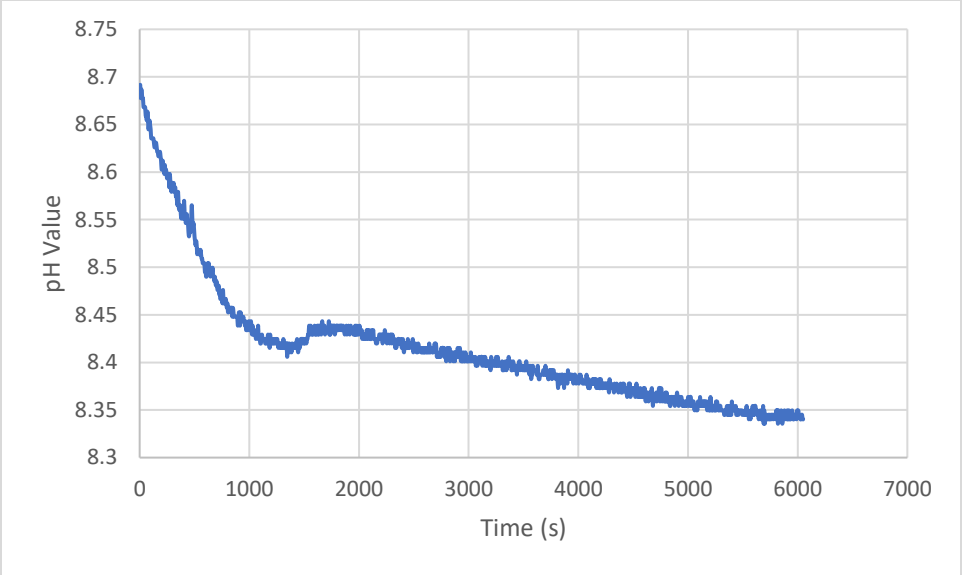

Figure S2 shows the pH versus time (s) recorded by the pH electrode during the titration run (10-6).

Figure S2 shows a slight decrease in the pH over time, indicating that the pH is not decreasing by substantial amounts (or that CO_2 is not interacting with the fluoride solution resulting in a decrease in pH).

Gebauer's 2008 experiment with calcium carbonate was reproducible, as similar n_{Ca}^{2+} (µmol) curves were able to be established.[11] The n_{Ca}^{2+} (µmol) data was shown to have lower n_{Ca}^{2+} values compared to the calculated total Ca^{2+} dosage line, indicating that calcium ions were binding to carbonate ions in solution. It is also important to note that cluster formation for calcium carbonate is more preferred at more alkaline pH levels (9-10). During the early titration runs, the n_{Ca}^{2+} La Mer[20] curve could not be replicated. This was mainly due to not bubbling helium gas into the reaction cell initially, which would have resulted in carbon dioxide reacting with the buffer solution (resulting in a decrease

in the pH). After bubbling helium gas into the solution, the n_{Ca}^{2+} curve for calcium carbonate could be produced.

The n_{Ca}^{2+} data for this experiment was in the shape of a La Mer curve, which confirmed the reproducibility of Gebauer et al's experiment.[11] As the n_{Ca}^{2+} curve reaches a peak, nucleation starts to occur to eventual crystal formation. At this point, there is a decrease in Gibbs energy for the reaction, due to the equilibrium being reached (for cluster formation).[11] The slope becomes negative after the peak due to the supersaturation of the solution and the decrease in Gibbs energy, where precipitation begins.

To further prove that Gebauer's experiment was reproducible, a laser pointer was used to shine the laser through the reaction cell. A small beam of light could be seen which indicated that particles were forming in solution (Tyndall effect).

Figures S3-S5 are the n_{Ca}^{2+} plot for calcium carbonate for Trials 1-3.

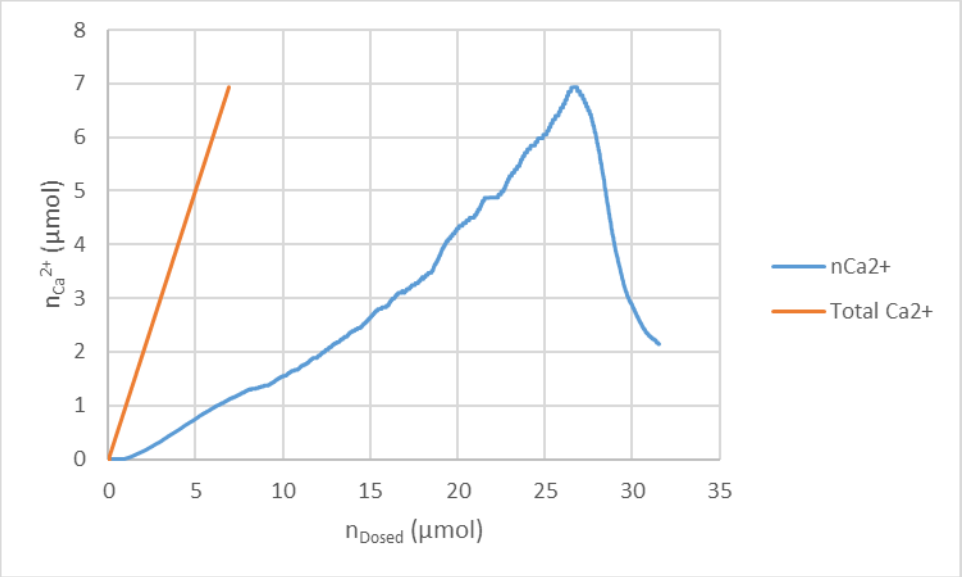

Figure S3 shows the n_{Ca}^{2+} (µmol) versus n_{Dosed} (µmol) (blue line) for the calcium carbonate titration. The total Ca^{2+} calculated by the flow rate is shown as well (orange line) for Trial 1.

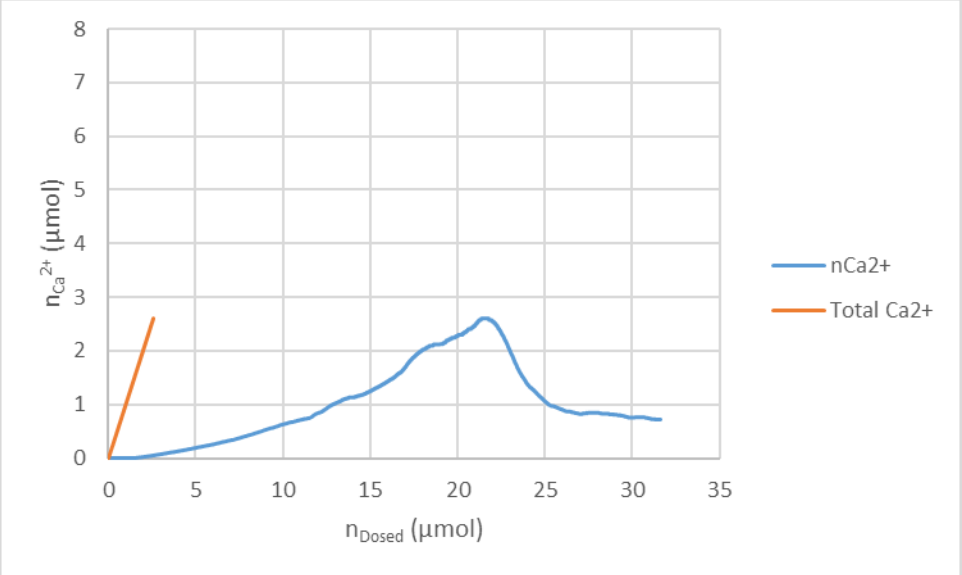

Figure S4 shows the n_{Ca}^{2+} (µmol) versus n_{Dosed} (µmol) (blue line) for the calcium carbonate titration. The total Ca^{2+} calculated by the flow rate is shown as well (orange line) for Trial 2.

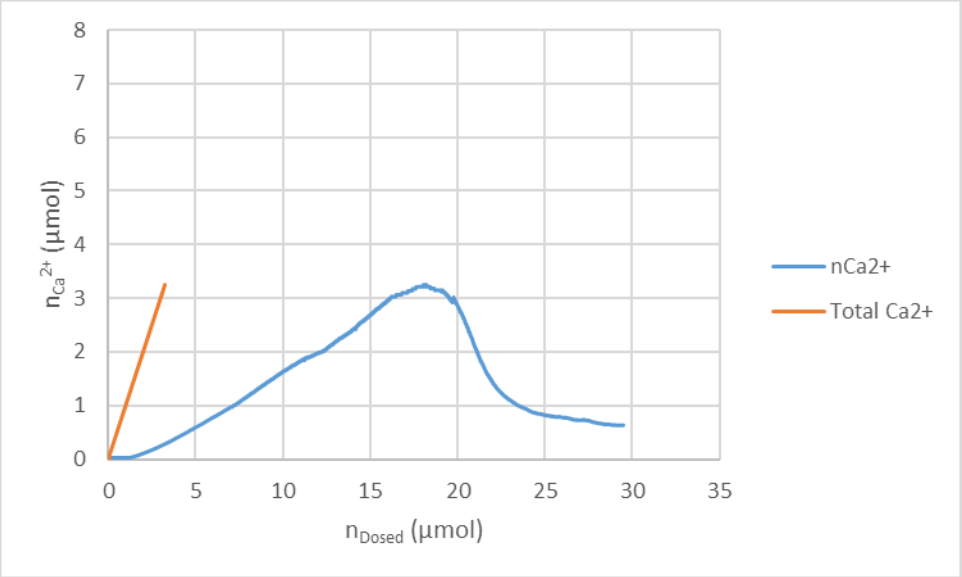

Figure S5 shows the n_{Ca}^{2+} (µmol) versus n_{Dosed} (µmol) (blue line) for the calcium carbonate titration. The total Ca^{2+} calculated by the flow rate is shown as well (orange line) for Trial 3.

Appendix B

Sample Calculations

Potential Data (mV) to n_{Ca}^{2+} (µmol)

The potential (mV) from the titration run had to be converted to n_{Ca}^{2+} (µmol) of the free calcium ions in solution. The potential data was first converted to the calculated calcium concentration (ppm). This was calculated by using the equation of the line from the calcium ISE calibration curve, plugging the potential data as *y* and solving for the calculated calcium concentration.

$$C_{Ca^{2+}}(ppm) = \left(\frac{y\ (mV) - b(mV)}{m\ (\frac{mV}{ppm})} \right)^{10}$$

Where C_{Ca}^{2+} *(ppm)* is the calculated calcium concentration, *y (mV)* is the potential data, *b (mV)* is the y-intercept from the equation of the line calibration plot, and *m (mV/ppm)* is the slope from the equation of the line. The calculated calcium concentration was then converted to amount of Ca^{2+} (g) by the equation below:

$$m_{Ca^{2+}}(g) = \left\{ \left[V_f(L) + \left(Q\ \left(\frac{L}{min}\right) x\ t\ (min) \right) \right] x\ C_{Ca^{2+}}(ppm) \right\}\ x\ \frac{1\ g}{1000\ mg}$$

Where m_{Ca}^{2+} *(g)* is the amount of calcium, V_f *(L)* is the volume of the fluoride solution, *Q (L/min)* is the flow rate of the titrant, and *t (min)* is the time. From there, the amount of calcium was then converted to n_{Ca}^{2+} (µmol):

$$n_{Ca^{2+}}\ (\mu mol) = \left(\frac{m_{Ca^{2+}}(g)}{MM\ (\frac{g}{mol})}\right) x\ \frac{1\ x\ 10^6\ \mu mol}{1\ mol}$$

Where $n_{Ca^{2+}}$ *(μmol)* is the $n_{Ca^{2+}}$ and *MM (g/mol)* is the molar mass for calcium (which is 40.078 g/mol). From there, the $n_{Ca^{2+}}$ plot was created as $n_{Ca^{2+}}$ (μmol) versus n_{Dosed} (μmol).

The total dosage Ca^{2+} line on the $n_{Ca^{2+}}$ plot was calculated to calculate what the $n_{Ca^{2+}}$ of free calcium ions should be based on the flow rate:

$$D_{Ca^{2+}}\ (\mu mol) = \left[\left(Q\ \left(\frac{L}{min}\right) x\ t\ (min)\right) x\ [Ca^{2+}](mM)\right] x\ \left(\frac{1000\ \mu mol}{1\ mmol}\right)$$

Where $D_{Ca^{2+}}$ *(μmol)* is the total Ca^{2+} dosage based on the flow rate and titrant concentration and *$[Ca^{2+}]$ (mM)* is the titrant volume.

Ion Pairing Calculations for CaF^+ and $CaCl^-$

Calculating for Quadratic Equation -

The following section includes the sample calculations that were used to determine if ion pairing (CaF^+) was an issue for the titration. First, the time (s) vs. $n_{Ca^{2+}}$ (μmol) of the titration and the dosage of Ca^{2+} had to be used for the calculations; the total dosage of Ca^{2+} (μmol) had to be converted to liters for further calculations.

$$V_{Ca^{2+}}\ (L) = \frac{[Q(\frac{mL}{\min})\ x\ t\ (\min)]}{1000\ mL/L}$$

Where the *total* $V_{Ca^{2+}}$ *(L)* is the calculated calcium dosage in liters, *Q (mL/min)* is the flow rate of the calcium solution, and the *t (min)* is the time of the titration. The initial $[Ca^{2+}]$ *(M)*, $[Ca^{2+}]_{initial}$, was calculated by the equation below:

$$[Ca^{2+}]_{initial}(M) = \left(\frac{[Ca^{2+}]\ (M) x\ V_{\ Ca^{2+}}\ (L)}{(V_F\ (L) +\ V_{Ca^{2+}}\ \ (L))}\right)$$

Where $[Ca^{2+}]$ *(M)* is the concentration of the titrant and the V_F *(L)* is the volume of fluoride solution in the reaction cell. The variable $[Ca^{2+}]_{initial}$ will be used to calculate the quadratic coefficients derived from the equilibrium equation for Ca^{2+}.

Ion Pairing Equilibrium Table –

First, an ICE table was constructed for the synthesis reaction for CaF^{+}:

$$Ca^{2+} + F^{-} \leftrightarrow CaF^{+}$$

Table S1 shows the ICE table for the reaction above:

Table S3 shows the ICE table for the synthesis reaction of CaF^+.

	Ca^{2+}	**F^-**	**CaF^+**
I	$[Ca^{2+}]$	$[F^-]$	0
C	- x	- x	+x
E	$[Ca^{2+}]$ - x	$[F^-]$ - x	+x

Where $[CaF^+]$ is the concentration for calcium monofluoride, $[Ca^{2+}]$ is the concentration for calcium, $[F^-]$ is the concentration for fluoride, and x is the change in the amount of one ion species. From there, the equilibrium equation for *K* was set up for the reaction:

$$4.805 = K = \frac{[CaF^+]}{[Ca^{2+}][F^-]}$$

Where *K* is the equilibrium constant for CaF^+ formation, $K = 10^{0.6817}$ or $K = 4.805$.[1] The terms from the E row in the ICE table were then substituted in the equilibrium equation:

$$4.805 = \frac{x}{([Ca^{2+}] - x)([F^-] - x)}$$

The next step was to set the equation to equal 0 and to solve for x:

$$4.805 = \frac{x}{([Ca^{2+}][F^-] - [Ca^{2+}]x - [F^-]x + x^2)}$$

$$4.805 = \frac{x}{\{x^2 - ([Ca^{2+}] + [F^-])x + ([Ca^{2+}][F^-])\}}$$

$$4.805\{x^2 - ([Ca^{2+}] + [F^-])x + ([Ca^{2+}][F^-])\} = x$$

$$4.805x^2 - (4.805([Ca^{2+}] + [F^-]))x + (4.805[Ca^{2+}][F^-]) = x$$

Subtracting *x* from both sides gives the equation below:

$$4.805x^2 + \left[\left(4.805(-[Ca^{2+}] - [F^-])\right)x - x\right] + (4.805[Ca^{2+}][F^-]) = 0$$

The above equation was used to determine the *a*, *b*, and *c* coefficients for the quadratic equation. The *a*, *b*, and *c* coefficients were determined below:

$$a = 4.805 \qquad b = [4.805(-[Ca^{2+}] - [F^-])x - x] \qquad c = (4.805[Ca^{2+}][F^-])$$

Solve x from Quadratic Equation –

The term *x* was calculated by using the calculated coefficients (*a*, *b* and *c*) and plugging them into the solution to the quadratic equation below:

$$\frac{-b \pm \sqrt{b^2 - 4ac}}{2a} = x$$

From the quadratic equation, two values for *x* are obtained from either adding or subtracting the square root*: x from quadratic (+) (M)* and *x* from *quadratic (-) (M)*. The latter term was chosen as the true value for *x* because the calculated *x* from the quadratic (+) (M) concentrations were physically unrealistic. It is important to note that *x* is denoted as [CaF^+].

Equilibrium [Ca^{2+}] and Plots –

With *x* from the quadratic equation (-) (M), the equilibrium concentration for $[Ca^{2+}]$, $[Ca^{2+}]_{eq}$ was calculated by subtracting *x* from the previous calculated initial $[Ca^{2+}]$ concentration.

$$[Ca^{2+}]eq\ (M) = [Ca^{2+}]_{inital}(M) - x\ (M)$$

From there, one plot was constructed showing $[Ca^{2+}]eq$ (M) versus time (s). Another plot of *x* ($[CaF^{+}]$) (M) versus time (s) was also constructed.

Ion Pairing with n_{Ca}^{2+} Plot –

For a n_{Ca}^{2+} plot the effect on ion pairing for the titration was calculated and observed. First, the *total volume (L), $V_{total,}$* of the reaction cell was calculated:

$$V_{total}\ (L) = V_{Ca^{2+}}\ (L) + 0.050\ L$$

Where the *total Ca^{2+} dosage (L)* was calculated earlier and 0.050 L is the amount of F^{-} solution in the reaction cell. Next, the equilibrium [CaF+], $n_{CaF^{+}}$, was converted to µmol:

$$n_{CaF^{+}}(\mu mol) = [x\ (M)\ x\ V_{total}\ (L)]\ x\ \left(\frac{1\ x\ 10^{6}\mu mol}{mol}\right)$$

After that, the amount of CaF^{+}, n_{CaF+} *(M),* was subtracted from the amount of Ca^{2+}, n_{Ca2+} *(eq) (µmol):*

$$nCa_{eq}^{2+}(\mu mol) = [([Ca^{2+}]_{initial}\ (M) -\ n_{CaF^{+}}(M)) * V_{total}\ (L)] * (\frac{1\ x\ 10^{6}\mu mol}{mol})]$$

Where n_{Ca}^{2+} is the amount of CaF^{+} (μmol) subtracted from the amount of Ca^{2+}. *$[Ca^{2+}]$ – x (μmol)* was then plotted versus the time of the titration in order to show the affect of ion pairing of the total Ca^{2+} dosage line (μmol). It can be determined that ion pairing is not a colossal issue in this experiment because of the small variation.

Calculate K –

In order to check the previous derivation, *K* was calculated for the reaction. First, the *corrected* $[Ca^{2+}]$ was calculated below:

$$[Ca^{2+}]_{eq}(M) = [Ca^{2+}]_{initial}(M) - x\ (M)$$

The equilibrium $[F^{-}]$ *(M)* was also calculated from subtracting the initial $[F^{-}]$ from *x (-) (M)* from the quadratic equation:

$$[F^{-}]_{eq}(M) = [F^{-}]_{initial}\ (M) - x\ (M)$$

The equilibrium constant *K* was calculated by using the equilibrium equation:

$$K = \frac{[CaF^{+}]_{eq}(M)}{[Ca^{2+}]_{eq}(M) \times\ [F^{-}]_{eq}(M)}$$

The value of *K* should equal to about 4.805, which is the literature value of *K* for CaF^{+}.

Ion pairing Calculations for $CaCl^{+}$ -

Ion pairing calculations were also done for $CaCl^{+}$ as well.

$$Ca^{2+} + Cl^{-} \leftrightarrow CaCl^{+}$$

The method of calculations for $CaCl^+$ was similar compared to CaF^+ except a few more calculations were used. The equilibrium constant equation for $CaCl^+$ can be written as below:

$$0.2016 = K = \frac{[CaCl^{+}]}{[Ca^{2+}][Cl^{-}]}$$

Where *K* is the equilibrium constant for $CaCl^+$, which is $K = 10^{-0.6956}$ or $K = 0.2016$.[1] The corrected $[Cl^-]$ had to be calculated for the ion pairing calculations:

$$[Cl^{-}]_{eq}(M) = \left\{\left[\left(\frac{D_{Ca^{2+}}(\mu mol)}{1\ x\ 10^{6}\left(\frac{\mu mol}{mol}\right)}\right)\ x\ \left(\frac{1}{V_{total}\ (L)}\right)\right] + [Cl]_{initial}(M)\right\}$$

Where $[Cl^-]_{eq}\ (M)$ is the corrected chloride, $D_{Ca^{2+}}\ (\mu mol)$ is the dosage of calcium, and $[Cl^-]_{initial}\ (M)$ is the initial chloride concentration.

Calculating K_{ip} for CaF^+

To further make sure that ion pairing was not a major factor in experimentation for calcium fluoride, the K_{ip} was calculated for CaF^+ using the $n_{Ca^{2+}}$ data. The first set of calculations were calculating the concentrations of Ca^{2+}, F^-, and CaF^+ with assuming only CaF^+ is being produced. The equations for calculating the concentrations of each ion species are shown below:

$$[Ca^{2+}](M) = \frac{\left(N_{Ca^{2+}}(\mu mol)\ x\ \frac{1\ mol}{1\ x\ 10^{6}\ \mu mol}\right)}{V_{total}(L)}$$

$$[CaF^{+}](M) = \left[\frac{\left([Ca^{2+}]_{titrant}\ x\ V_{Ca^{2+}}(L)\right)}{V_{total}(L)}\right] - [Ca^{2+}](M) + [Ca^{2+}]_{corrected}(M)$$

$$[F^{-}](M) = \left[\frac{\left([F^{-}]_{inital}(M)\ x\ L_{F^{-}}(L)\right)}{V_{total}(L)}\right] - [CaF^{+}](M)$$

Where *$[Ca^{2+}]$ (M)*, *$[CaF^{+}]$ (M)*, and *$[F^{-}]$ (M)* are the calculated concentrations of each ion species and *$[Ca^{2+}]_{corrected}$ (M)* was a correction in excel made when treating the other variables in the calculation (using dollar signs for $[Ca^{2+}]$). Before calculating the K_{ip}, the ionic strength and activities for each species had to be calculated. The ion strength calculation is shown below:

$$\mu = \frac{1}{2}\sum c_i, z_i^2$$

Where μ is the ionic strength, c_i *(M)* is the concentration of the ion species, and z_i is the charge of the same ion. The activity of each ion species was also calculated by using the extended Debye-Hückel equation, which is shown below:

$$\log\gamma = \frac{-0.51z^2\sqrt{\mu}}{1 + \left(\frac{\alpha\sqrt{\mu}}{305}\right)}$$

Where γ is the activity for an ion species, z is the charge, and α *(pm)* is the ion size. The activity for each ion species was included in calculating K_{ip} for CaF^{+}:

$$K_{ip} = \frac{\gamma_{CaF^+}[CaF^+]}{\gamma_{Ca^{2+}}[Ca^{2+}]\gamma_{F^-}[F^-]}$$

Where γ_{CaF+}, γ_{Ca2+}, and γ_{F-} are the activities of each ion species. From there, a plot was created of K_{ip} versus time (s) for each n_{Ca}^{2+} plot (prior to the nucleation point) and the average K_{ip} was calculated before the nucleation point.

Appendix B

Reference

(1) Johnson J.; Anderson F.; Parkhurst D.L. Database thermo.com.V8.R6.230, Rev 1.11. Lawrence Livermore National Laboratory, Livermore, California, **2000**.

Appendix C

Other Data Plots for Calcium Fluoride

Calibration Curve for Calcium Fluoride Experiments

A calibration curve was constructed for each experiment by measuring the potential of the calcium standards versus standard concentration shown by Figure S6. The equation of the trend line was used for n_{Ca}^{2+} calculations.

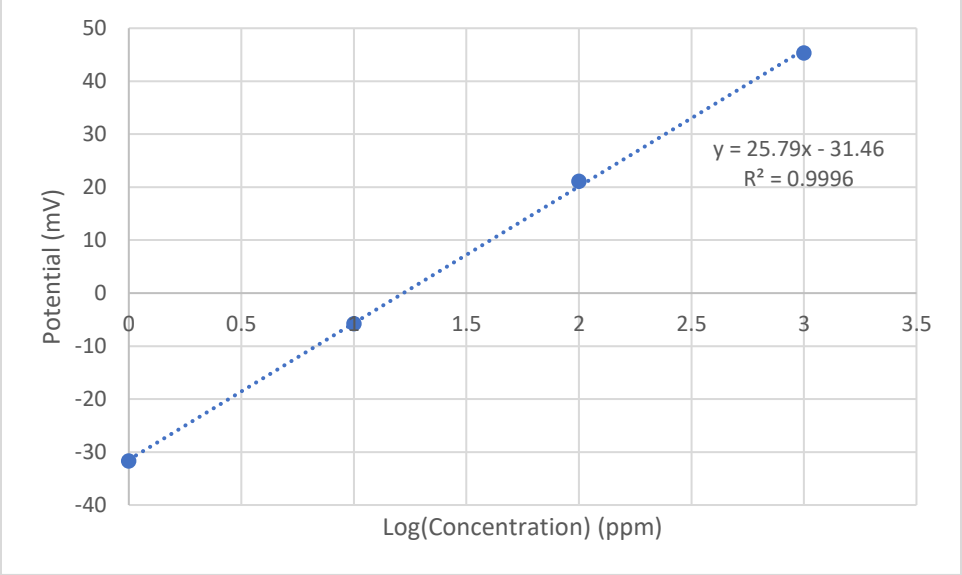

Figure S6 shows the calibration curve of potential (mV) versus log(concentration) (ppm) for the calcium fluoride experiment for [F^-] = 25.6 mM, Trial 1.

Measured pH for Calcium Fluoride Experiment

The pH was recorded versus time for each calcium fluoride experiment, one example is shown by Figure S7 below. The calculated pH for the experiment (based on remaining F^- in the solution) is also shown.

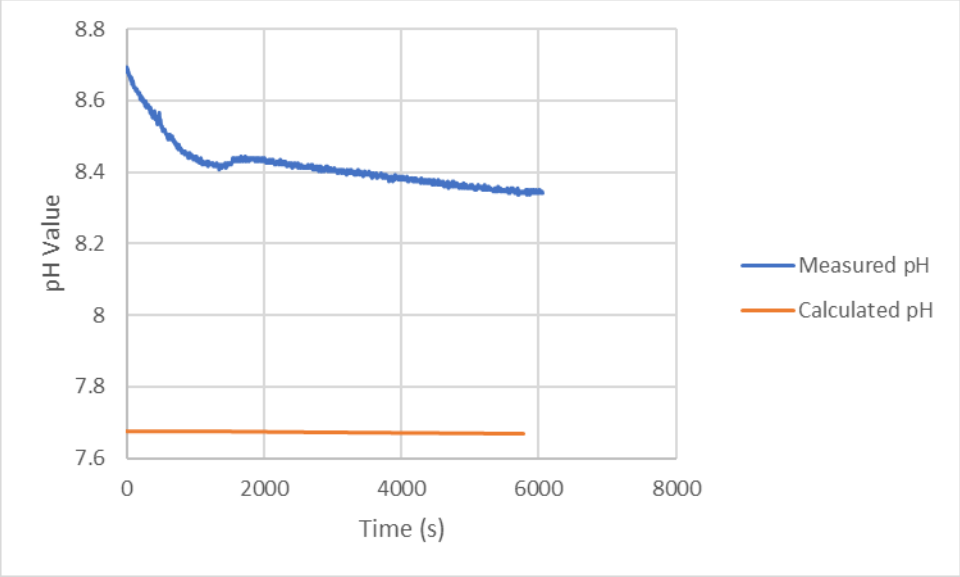

Figure S7 shows the pH versus time (s) for the calcium fluoride experiment for [F^-] = 25.6 mM, Trial 1.

Figure shows that the drop in the measured pH is not explained by the loss of F^- in the reaction cell.

n_{Ca}^{2+} Curves for Calcium Fluoride Experiments

Figures S8-S21 consist of n_{Ca}^{2+} plots for calcium fluoride at the specified concentrations. A triplicate run was performed for each [F^-].

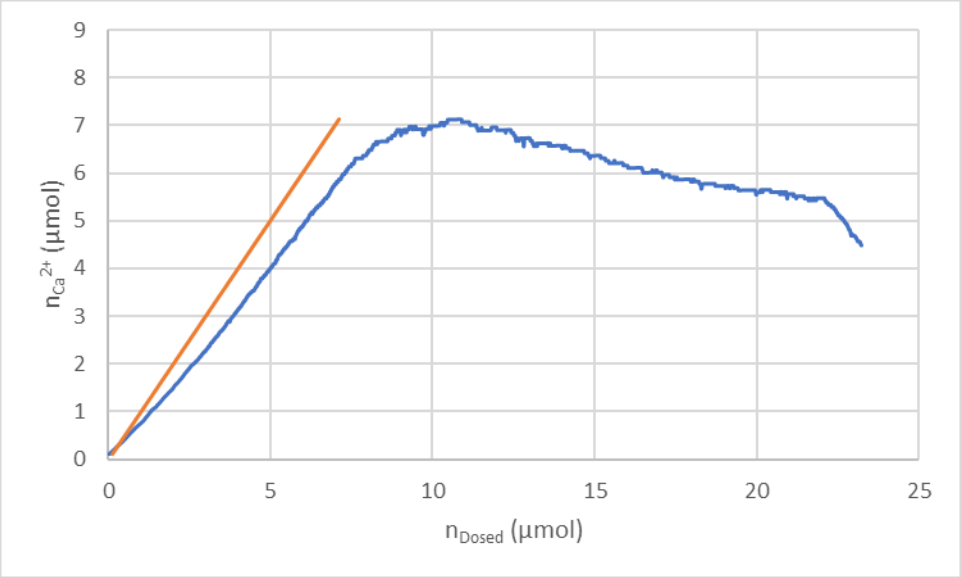

Figure S8 shows the n_{Ca}^{2+} of free calcium ions (µmol) versus n_{Dosed} (µmol) for the titration (blue line). The total calcium based on the flow rate is also shown (orange line). This was done at $[F^-]$ = 12.8 mM, Trial 1.

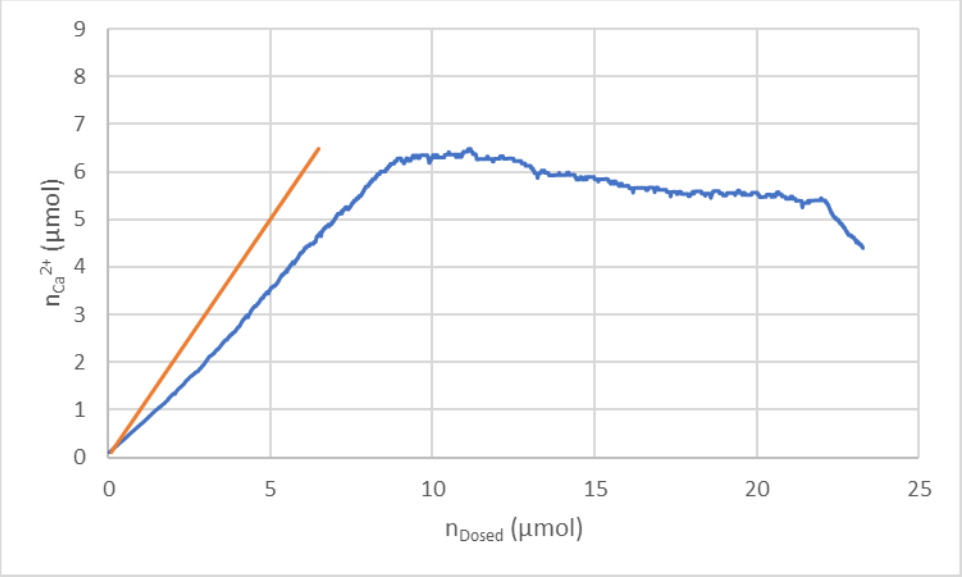

Figure S9 shows the n_{Ca}^{2+} of free calcium ions (µmol) versus n_{Dosed} (µmol) for the titration (blue line). The total calcium based on the flow rate is also shown (orange line). This was done at $[F^-]$ = 12.8 mM, Trial 2.

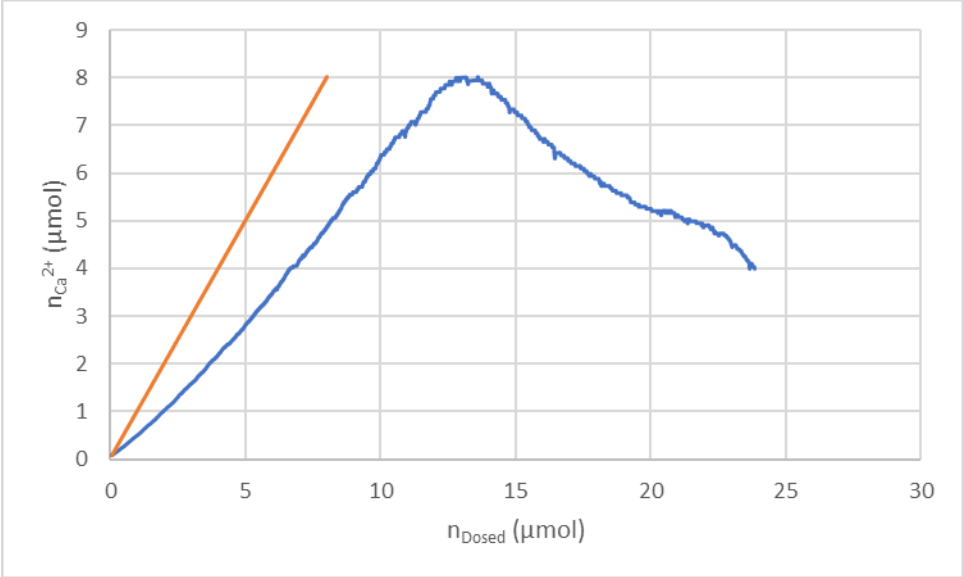

Figure S10 shows the n_{Ca}^{2+} of free calcium ions (µmol) versus n_{Dosed} (µmol) for the titration (blue line). The total calcium based on the flow rate is also shown (orange line). This was done at [F^-] = 12.8 mM, Trial 3.

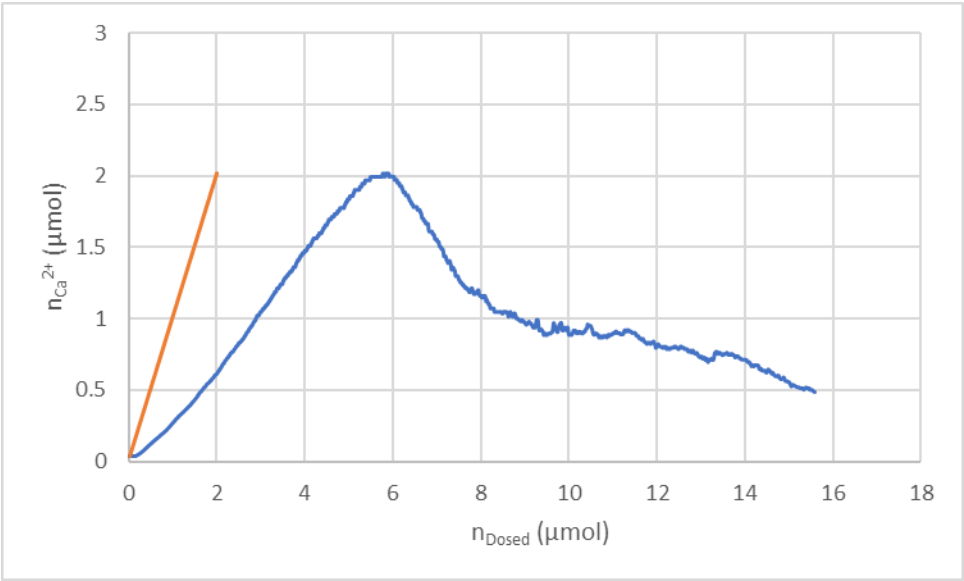

Figure S11 shows the n_{Ca}^{2+} of free calcium ions (µmol) versus n_{Dosed} (µmol) for the titration (blue line). The total calcium based on the flow rate is also shown (orange line). This was done at [F^-] = 25.6 mM, Trial 2.

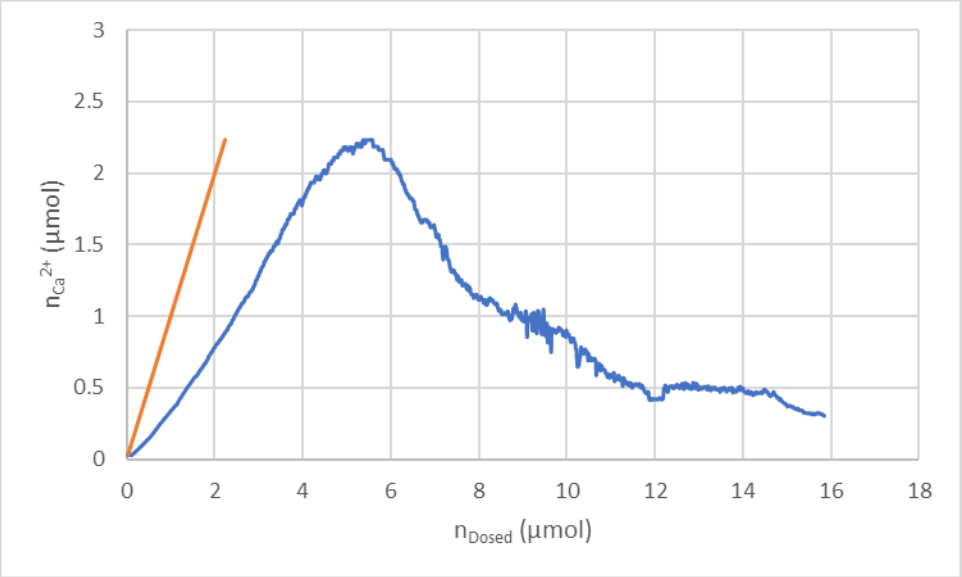

Figure S12 shows the n_{Ca}^{2+} of free calcium ions (µmol) versus n_{Dosed} (µmol) for the titration (blue line). The total calcium based on the flow rate is also shown (orange line). This was done at [F^-] = 25.6 mM, Trial 3.

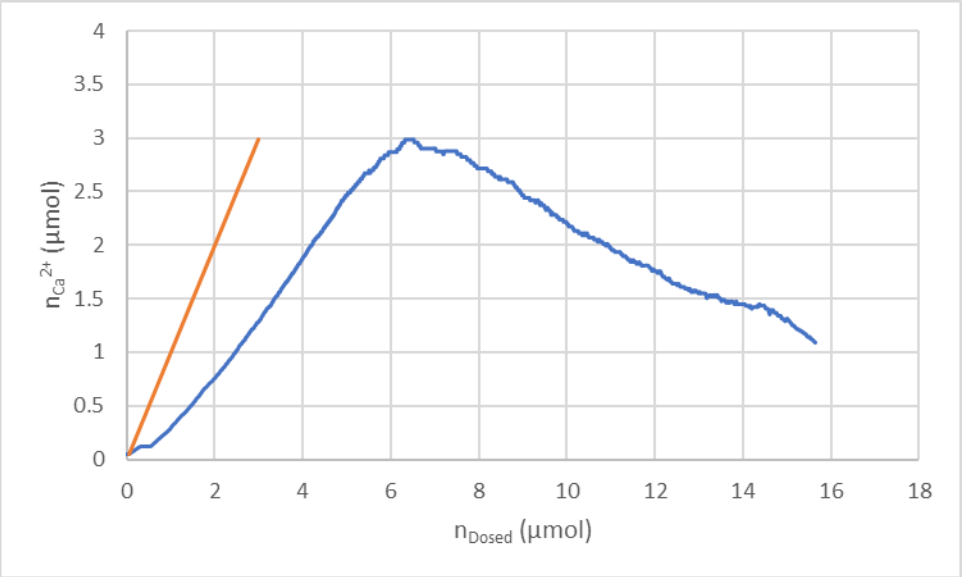

Figure S13 shows the n_{Ca}^{2+} of free calcium ions (µmol) versus n_{Dosed} (µmol) for the titration (blue line). The total calcium based on the flow rate is also shown (orange line). This was done at [F^-] = 19.2 mM, Trial 1.

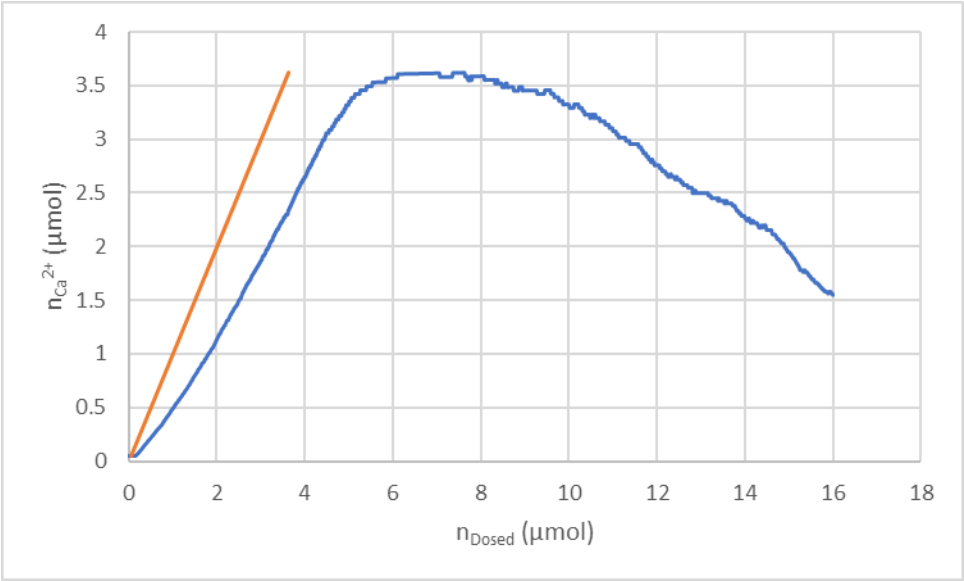

Figure S14 shows the n_{Ca}^{2+} of free calcium ions (µmol) versus n_{Dosed} (µmol) for the titration (blue line). The total calcium based on the flow rate is also shown (orange line). This was done at $[F^-]$ = 19.2 mM, Trial 2.

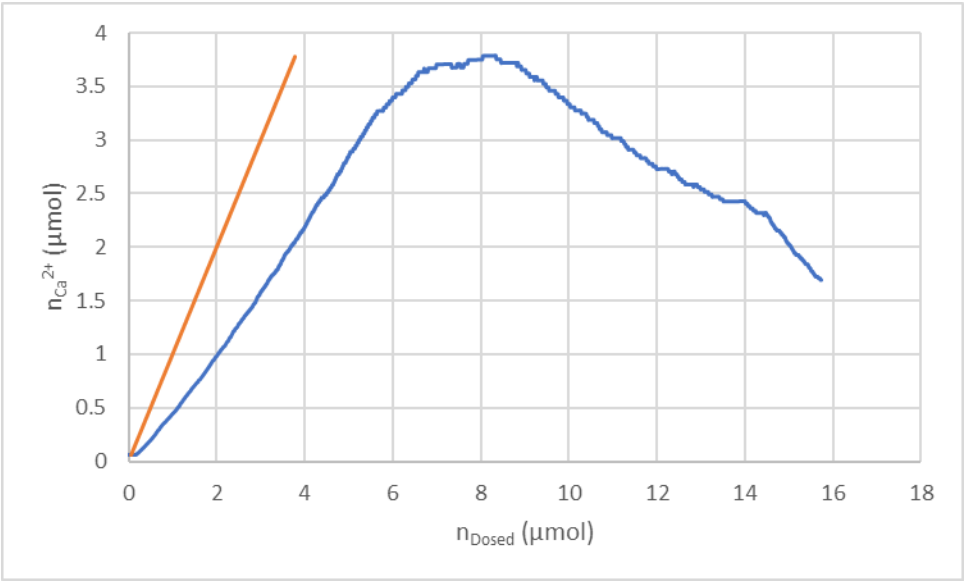

Figure S15 shows the n_{Ca}^{2+} of free calcium ions (µmol) versus n_{Dosed} (µmol) for the titration (blue line). The total calcium based on the flow rate is also shown (orange line). This was done at $[F^-]$ = 19.2 mM, Trial 3.

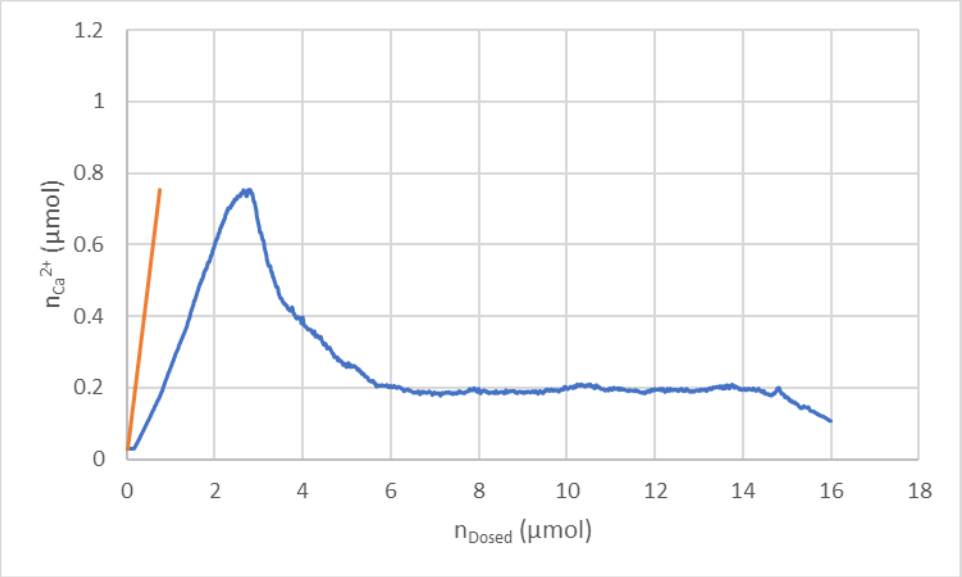

Figure S16 shows the n_{Ca}^{2+} of free calcium ions (µmol) versus n_{Dosed} (µmol) for the titration (blue line). The total calcium based on the flow rate is also shown (orange line). This was done at $[F^-]$ = 38.4 mM, Trial 1.

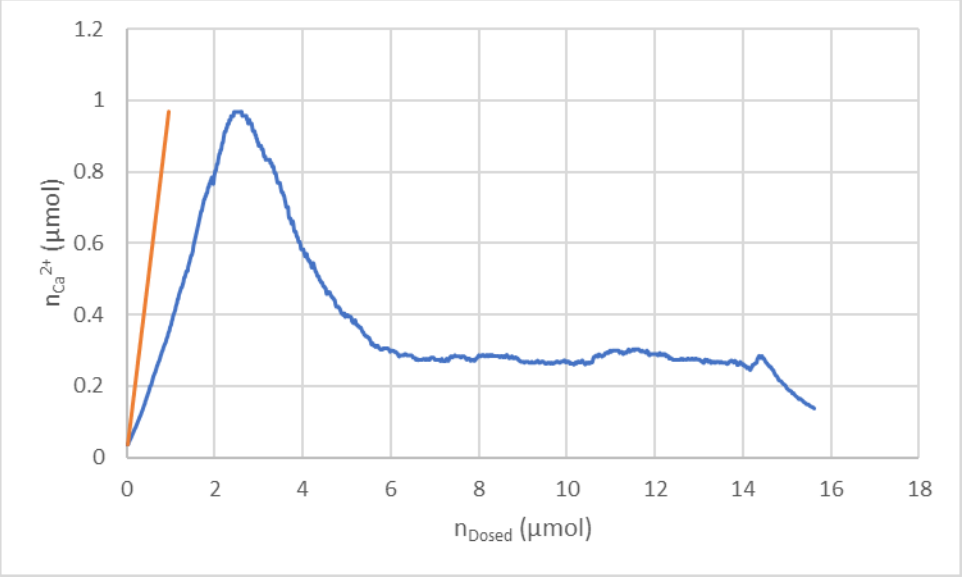

Figure S17 shows the n_{Ca}^{2+} of free calcium ions (µmol) versus n_{Dosed} (µmol) for the titration (blue line). The total calcium based on the flow rate is also shown (orange line). This was done at $[F^-]$ = 38.4 mM, Trial 2.

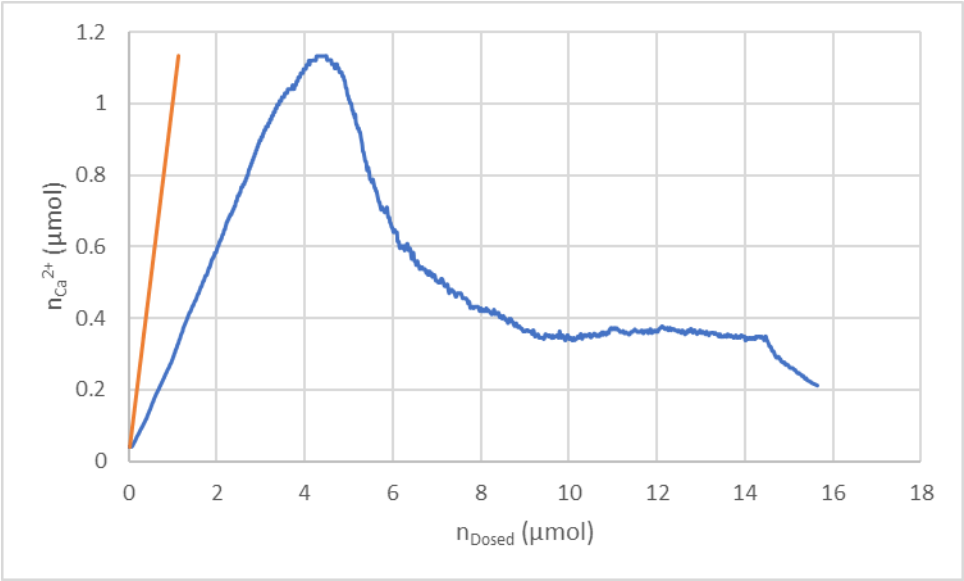

Figure S18 shows the n_{Ca}^{2+} of free calcium ions (µmol) versus n_{Dosed} (µmol) for the titration (blue line). The total calcium based on the flow rate is also shown (orange line). This was done at $[F^-]$ = 38.4 mM, Trial 3.

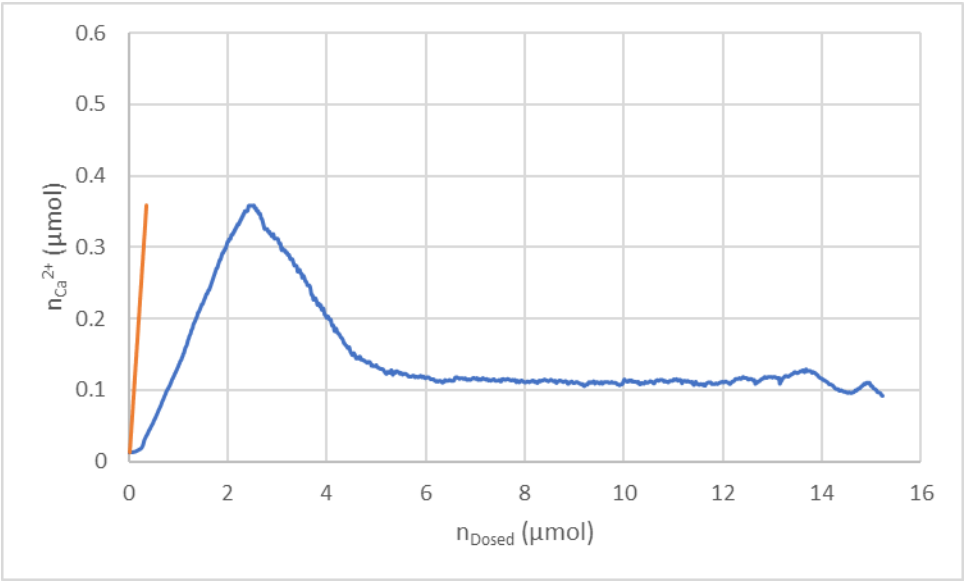

Figure S19 shows the n_{Ca}^{2+} of free calcium ions (µmol) versus n_{Dosed} (µmol) for the titration (blue line). The total calcium based on the flow rate is also shown (orange line). This was done at $[F^-]$ = 51.2 mM, Trial 1.

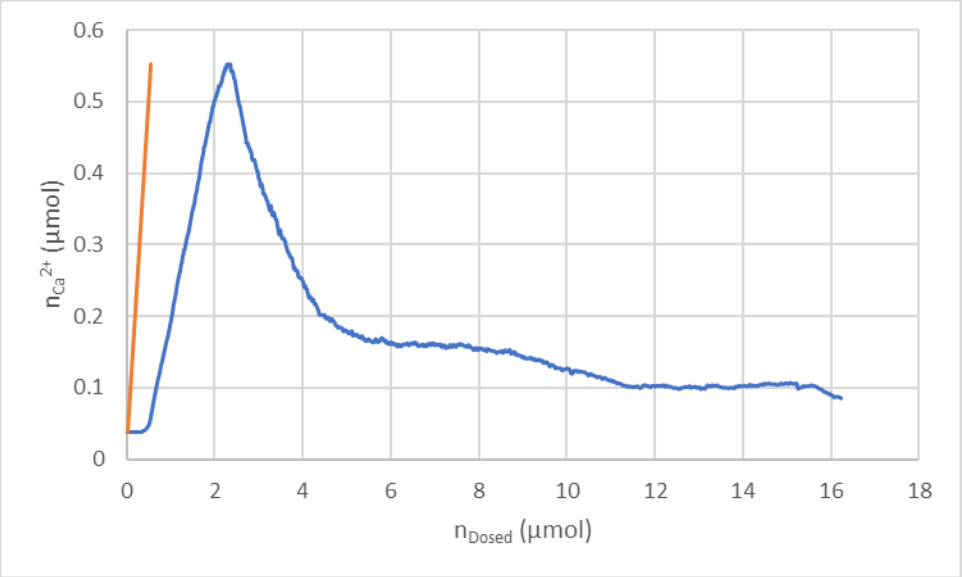

Figure S20 shows the n_{Ca}^{2+} of free calcium ions (µmol) versus n_{Dosed} (µmol) for the titration (blue line). The total calcium based on the flow rate is also shown (orange line). This was done at $[F^-]$ = 51.2 mM, Trial 2.

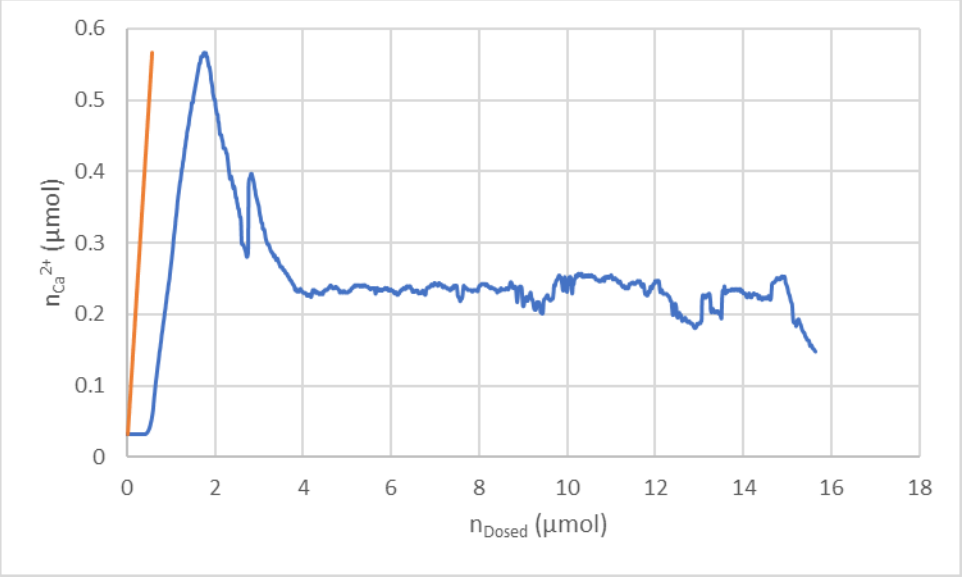

Figure S21 shows the n_{Ca}^{2+} of free calcium ions (µmol) versus n_{Dosed} (µmol) for the titration (blue line). The total calcium based on the flow rate is also shown (orange line). This was done at $[F^-]$ = 51.2 mM, Trial 3.

Triplicate plots for Calcium Fluoride Experiment

The n_{Ca}^{2+} data for Figures S22-S25 performed was plotted with all three n_{Ca}^{2+} curves together to construct triplicate plots for the other fluoride concentrations.

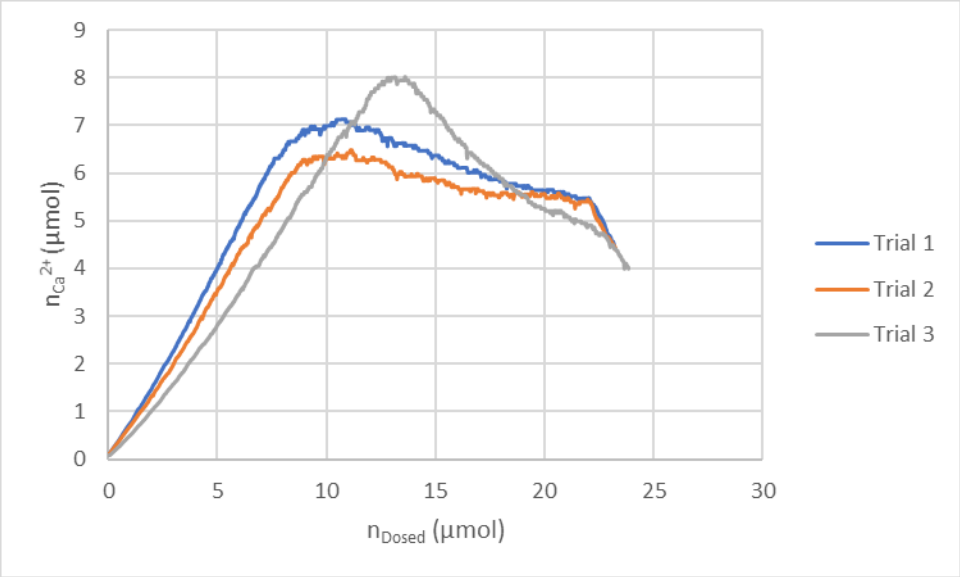

Figure S22 shows the n_{Ca}^{2+} (µmol) vs. n_{Dosed} (µmol) for a triplicate run for [F^-] = 12.8 mM.

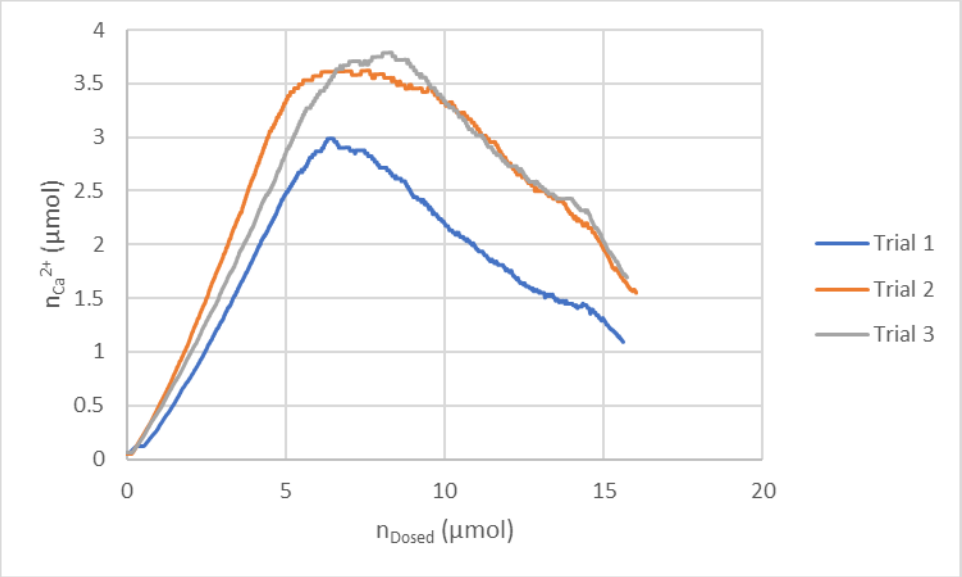

Figure S23 shows the n_{Ca}^{2+} (µmol) vs. n_{Dosed} (µmol) for a triplicate run for $[F^-]$ = 19.2 mM.

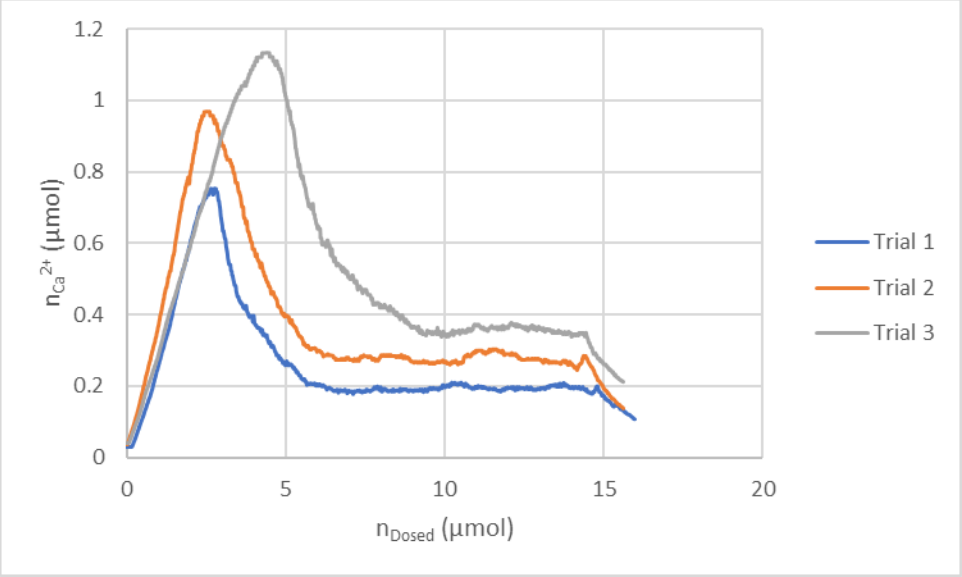

Figure S24 shows the n_{Ca}^{2+} (µmol) vs. n_{Dosed} (µmol) for a triplicate run for $[F^-]$ = 38.4 mM.

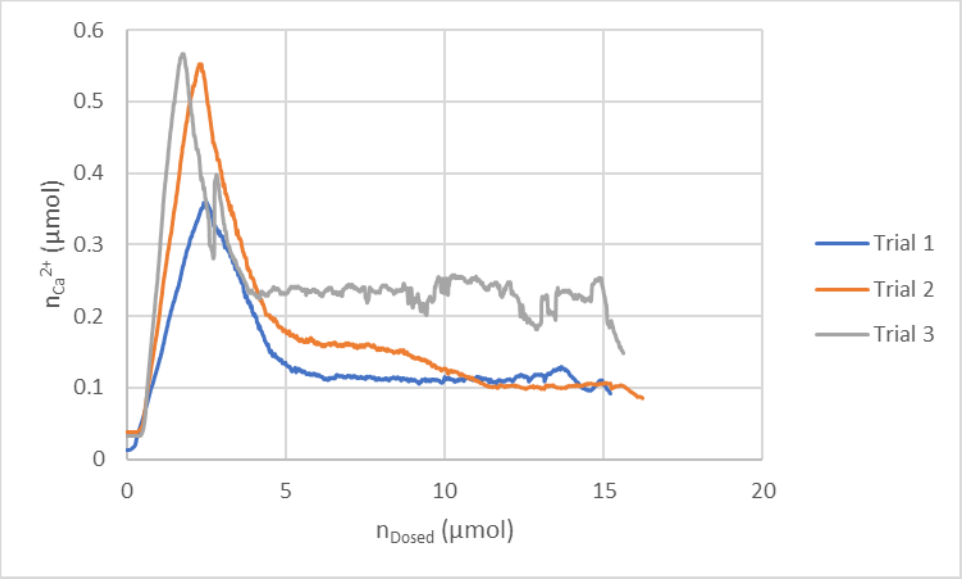

Figure S25 shows the $n_{Ca^{2+}}$ (µmol) vs. nDosed (µmol) for a triplicate run for [F^-] = 51.2 mM.

K_{ip} plots for Calcium Fluoride Experiment (CaF^+)

The calculated K_{ip} was plotted versus time (s) for each experiment prior to the nucleation peak of the reaction cell, which are shown by Figures S26-S37 below.

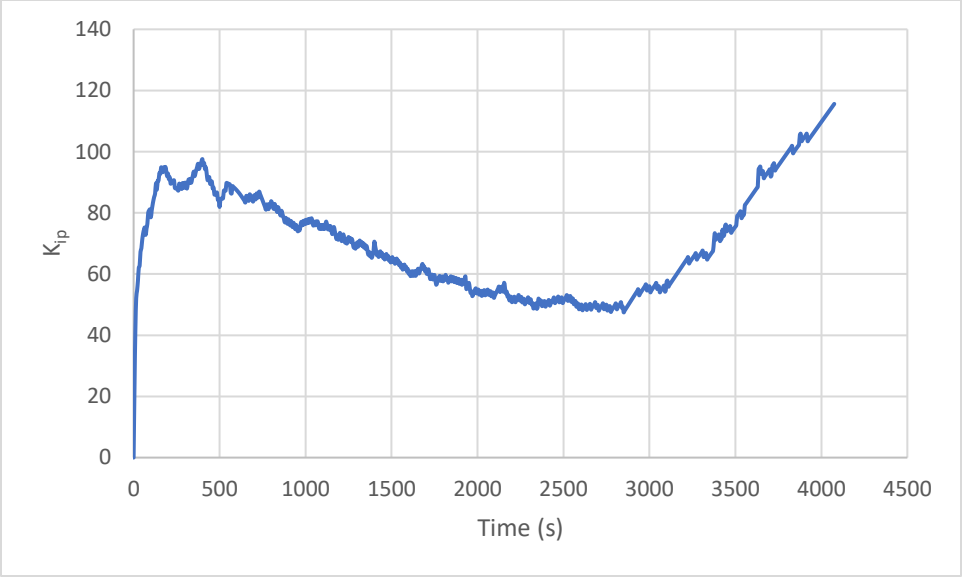

Figure S26 shows the K_{ip} for CaF^+ versus time (s) for the calcium fluoride titration for $[F^-]$ = 12.8 mM, Trial 1.

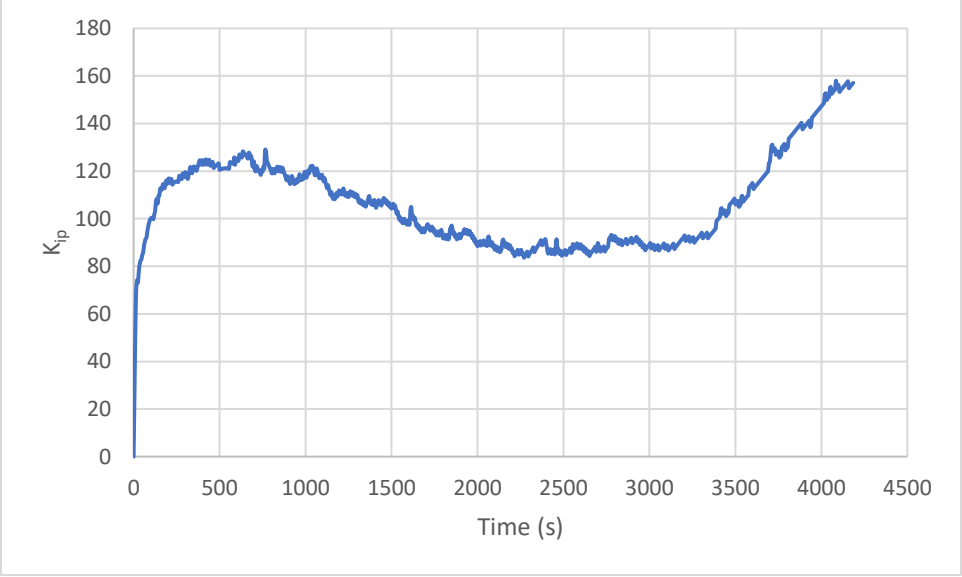

Figure S27 shows the K_{ip} for CaF^+ versus time (s) for the calcium fluoride titration for $[F^-]$ = 12.8 mM, Trial 2.

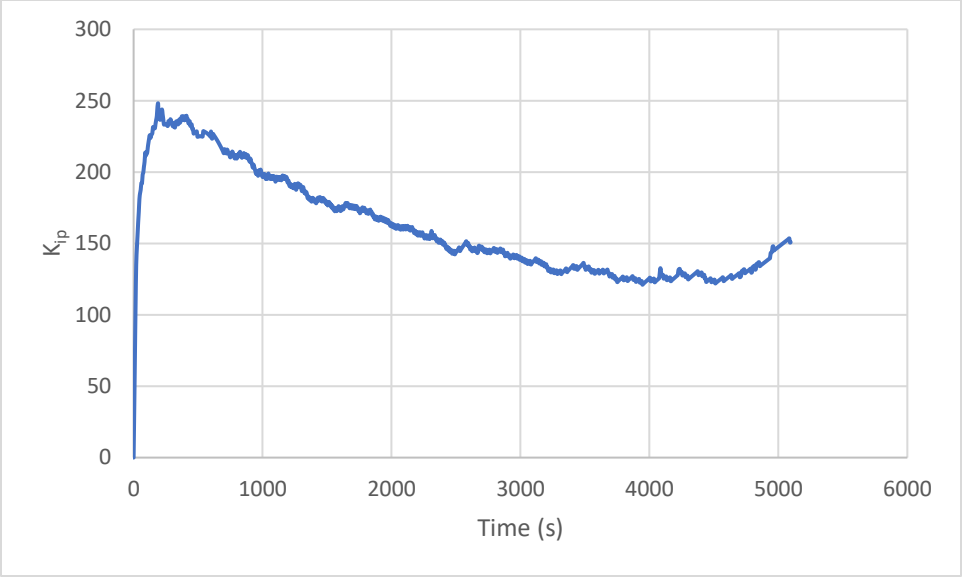

Figure S28 shows the K_{ip} for CaF^+ versus time (s) for the calcium fluoride titration for $[F^-]$ = 12.8 mM, Trial 3.

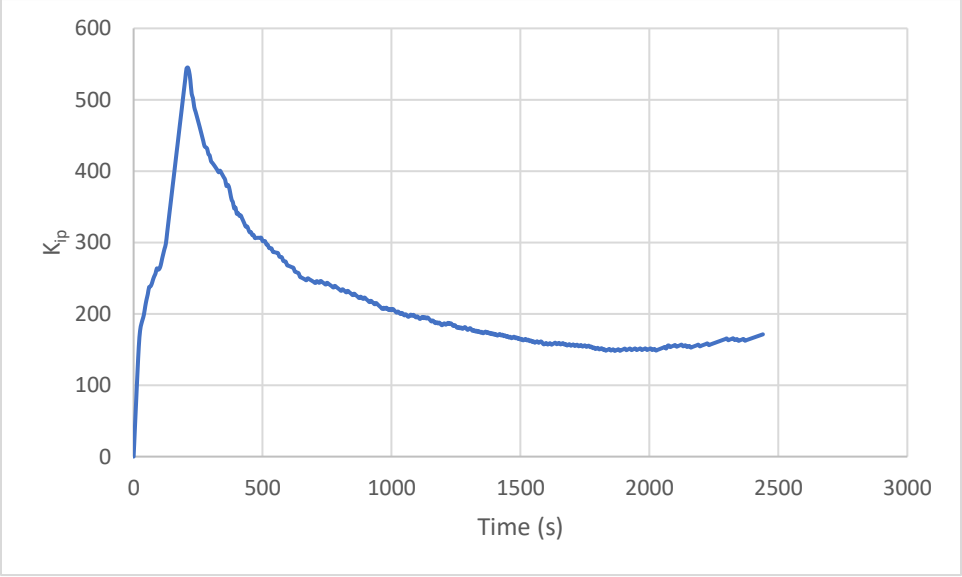

Figure S29 shows the K_{ip} for CaF^+ versus time (s) for the calcium fluoride titration for $[F^-]$ = 19.2 mM, Trial 1.

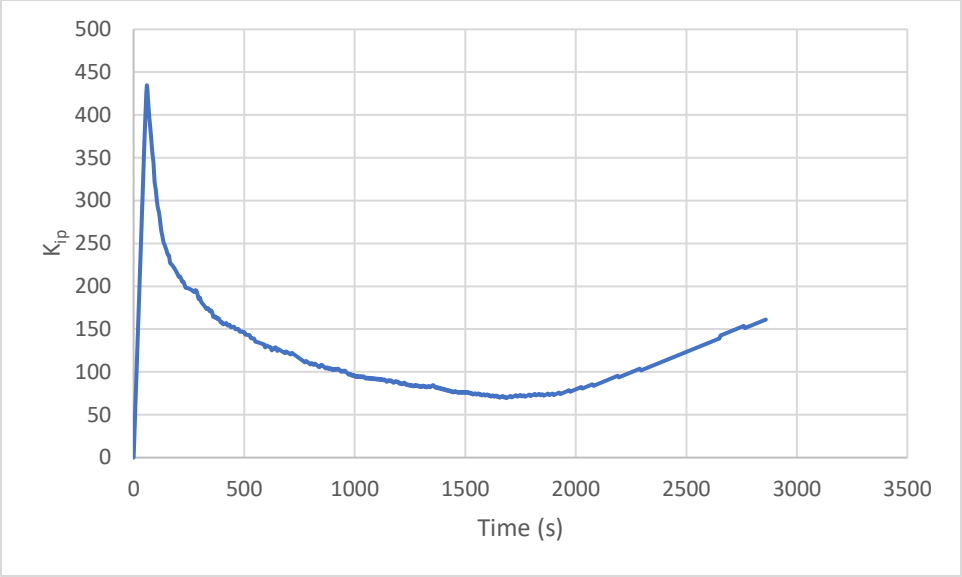

Figure S30 shows the K_{ip} for CaF^+ versus time (s) for the calcium fluoride titration for $[F^-]$ = 19.2 mM, Trial 2.

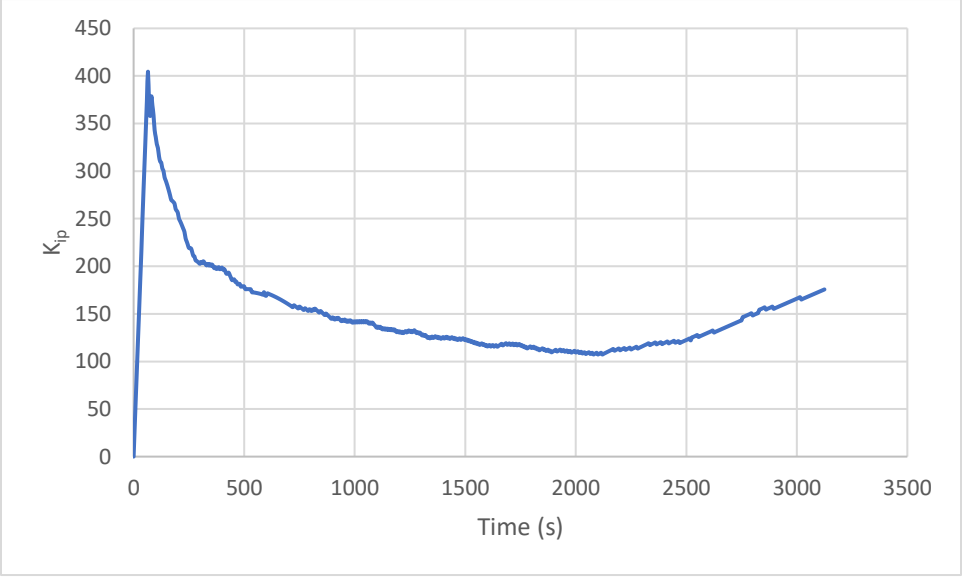

Figure S31 shows the K_{ip} for CaF^+ versus time (s) for the calcium fluoride titration for $[F^-]$ = 19.2 mM, Trial 3.

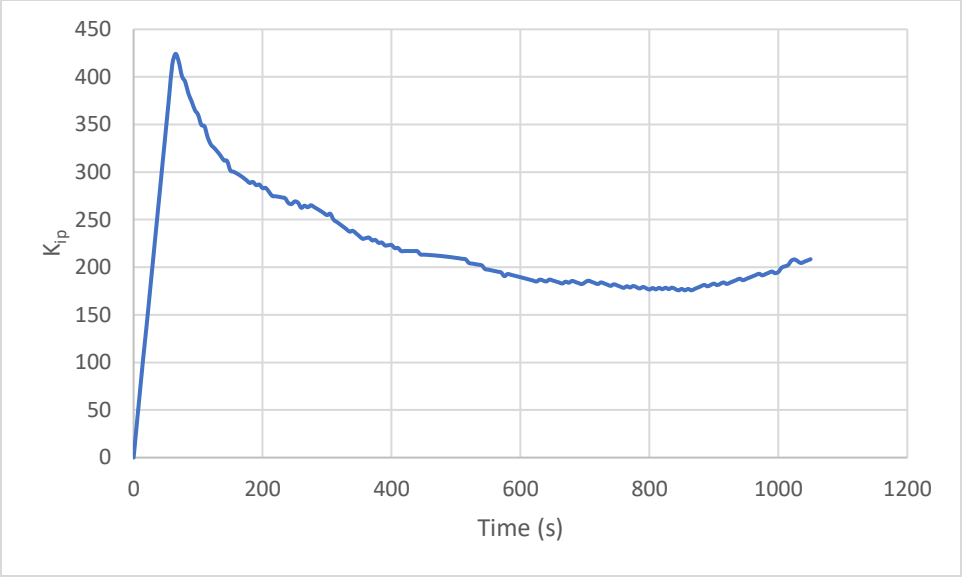

Figure S32 shows the K_{ip} for CaF^+ versus time (s) for the calcium fluoride titration for $[F^-]$ = 38.4 mM, Trial 1.

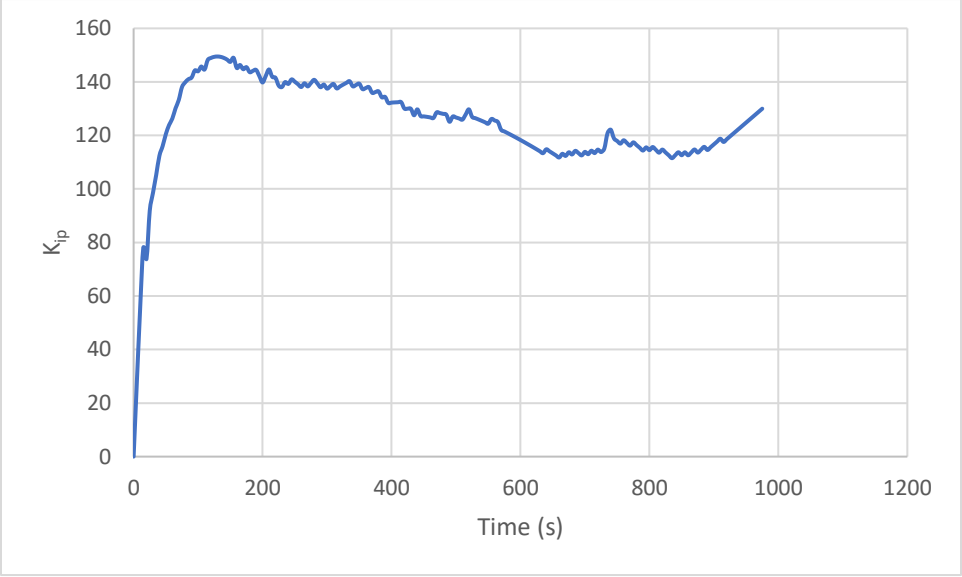

Figure S33 shows the K_{ip} for CaF^+ versus time (s) for the calcium fluoride titration for $[F^-]$ = 38.4 mM, Trial 2.

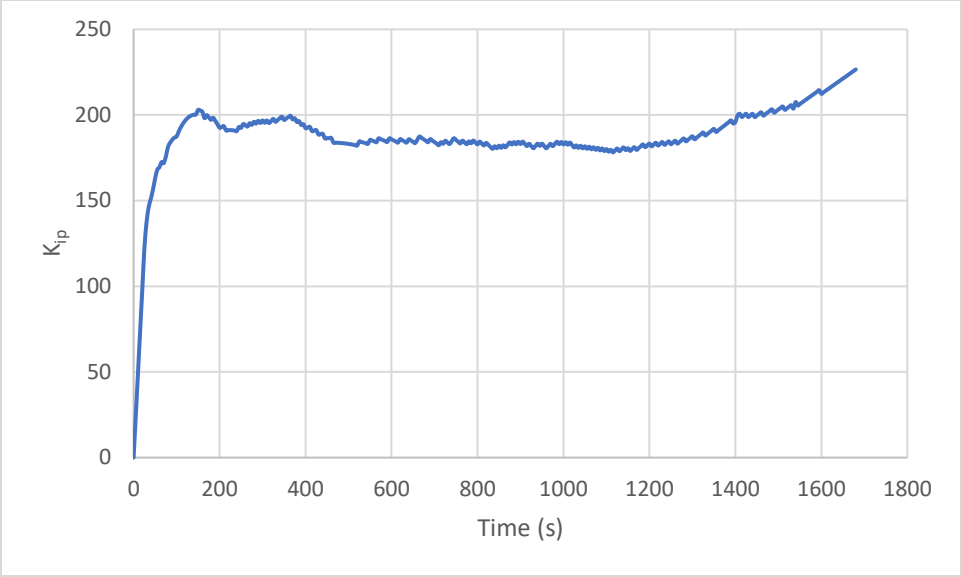

Figure S34 shows the K_{ip} for CaF^+ versus time (s) for the calcium fluoride titration for $[F^-]$ = 38.4 mM, Trial 3.

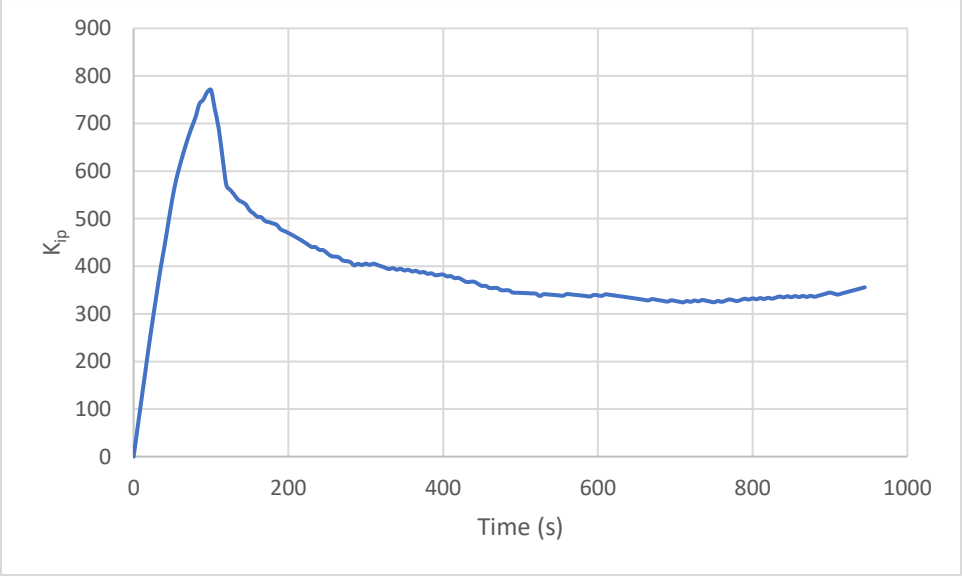

Figure S35 shows the K_{ip} for CaF^+ versus time (s) for the calcium fluoride titration for $[F^-]$ = 51.2 mM, Trial 1.

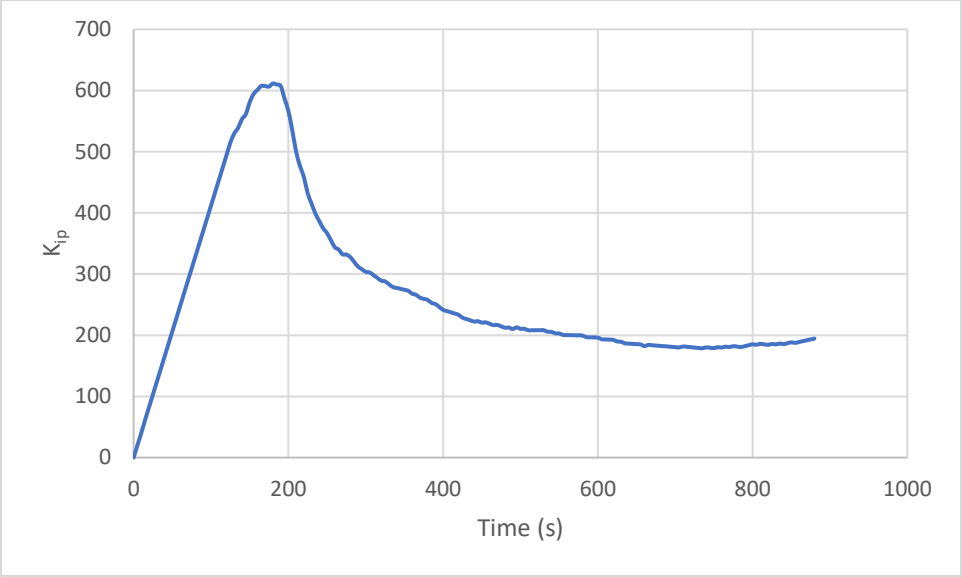

Figure S36 shows the K_{ip} for CaF^+ versus time (s) for the calcium fluoride titration for $[F^-]$ = 51.2 mM, Trial 2.

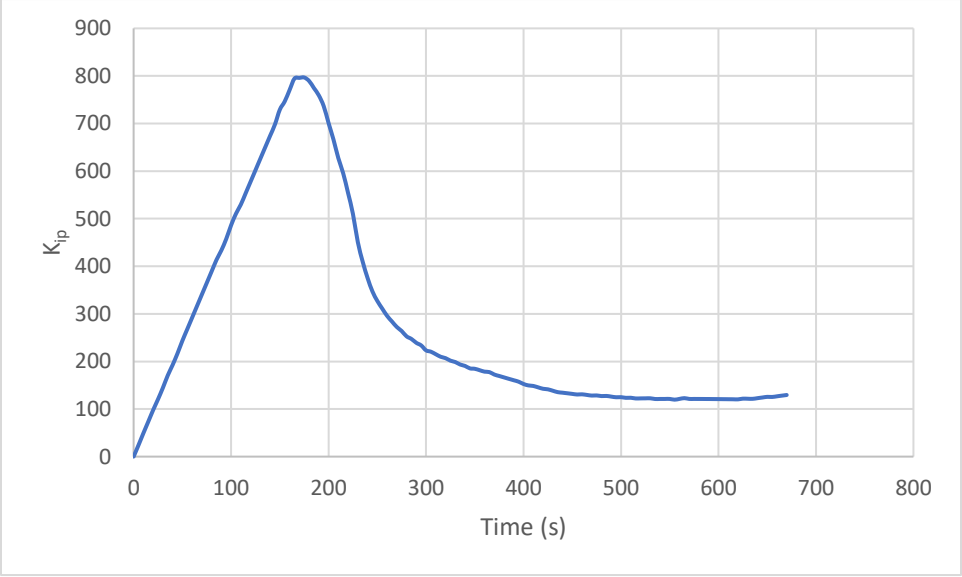

Figure S37 shows the K_{ip} for CaF^+ versus time (s) for the calcium fluoride titration for $[F^-]$ = 51.2 mM, Trial 3.

Appendix D

Laser Pointer Experiment for Calcium Fluoride

A laser pointer was lighted and pointed through the reaction cell after the titration experiment and through a beaker of HQ water as shown by Figures S38 and S39.

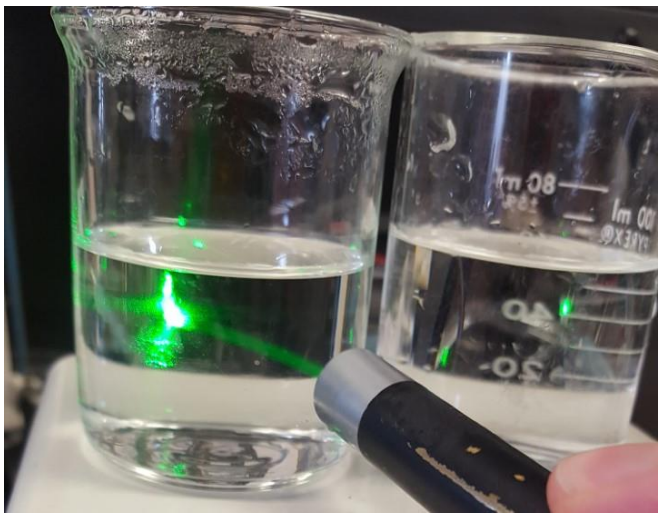

Figure S38 shows the laser pointer experiment for calcium fluoride ([F^-] = 12.8 mM) where the laser is being pointed at the reaction cell.

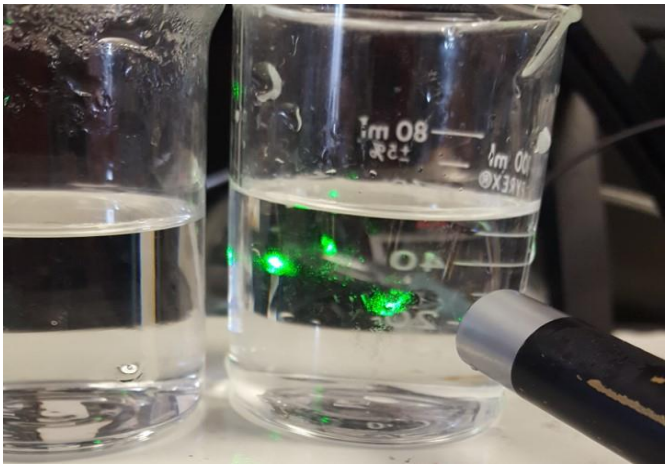

Figure S39 shows the laser pointer experiment for calcium fluoride ([F^-] = 12.8 mM) where the laser is being pointed at the HQ water.